Structural Health Monitoring – Its Association and Use

Christian Boller [*‡]

[*] Chair in NDT and Quality Assurance, Saarland University, Saarbrücken/Germany

[‡] Fraunhofer Institute for Nondestructive Testing, Dresden & Saarbrücken/Germany

Abstract Structural Health Monitoring (SHM) is an expression being around for more than two decades now. Triggered by damage tolerant design where damage has to be inspected at defined intervals based on non-destructive testing (NDT) techniques modern sensing hardware may now be integrated into structural materials and combined with advanced signal processing software making NDT to become an integral part of materials and structures and hence conventional inspection processes to be automated. This chapter provides an insight into the background of and the motivation for SHM by describing needs and assumptions made when designing a damage tolerant structure. It explains the need for loads monitoring and the implications those loads have on damage such as fatigue propagating during a structure's operational life. NDT techniques with a specific potential for SHM are addressed including their impact on monitoring carbon-fibre reinforced composites being one of the different material types where SHM plays a significant role. Finally some outlook is made with regard to SHM implementation and the benefits to be gained where examples have been taken from aviation and some outlook is provided considering SHM applications in wind energy generation.

1 A Motivation for Structural Health Monitoring

Engineering structures today are continuously ageing, would those be in civil engineering, energy generation or aeronautics, to just name a few. Civil engineering buildings such as houses or bridges are not truly designed for a finite life, although one is aware that those will not last forever. In nuclear energy generation there is currently a significant discussion ongoing with regard to life extension of existing power plants which also stems from the fact that many of the power plants have been used less than they were

W. Ostachowicz, J. Güemes (Eds.), *New Trends in Structural Health Monitoring*, CISM International Centre for Mechanical Sciences, DOI 10.1007/978-3-7091-1390-5_1,

expected to be used. This is characteristic with regard to many of the high asset values a society has, where any extension of an initially assumed operational life is a potential benefit to the operator.

An area where usage is often higher than expected can be seen with road transportation and its related infrastructure. The increased number of vehicles as well as vehicle loads in general has increased deterioration of road tarmacs and bridges, to just name a few. This has again resulted in increased inspection and maintenance effort required to keep those structures operational since cost for replacement of those buildings will rather exceed resources being available, would those be related to material, people or funding in general. The big challenge in managing the criticality of a structure is therefore the determination of a structure's current damage condition even in a quantifiable manner. This quantification requires an in depth understanding of a material's and structure's damage condition, which is currently still quite difficult although a lot of know how being present.

An observation similar to the civil engineering sector can be made with aircraft. Aircraft are engineering structures well designed from an engineering point of view. Due to their complexity in structural design as well as in operation aircraft do contain a variety of components as well as loading conditions which can lead to damage to occur during in service operation. This damage is quantitatively covered during roughly the first half of an aircraft's operational life, specifically in terms of damage tolerant design. However when it comes to the second half of those aircrafts' lives a lot of damages do occur which have not been anticipated in the aircraft's initial design and which have to be covered by a variety of additional inspections and possibly even modifications. One of the most challenging aircraft types in that regard is the Boeing B-52 bomber, which has been designed and built shortly after World War II and is due to stay in operation until the year 2045. Any modification to be done on this type of aircraft today – where there are still sufficient to be expected – does suffer from the lack of knowledge in the structural design of those old structures as well as in the degree an individual structure has truly aged. Means of identifying such a structure's degree of damage are therefore very much in need.

Aircraft are also very much prone to accidental damage, mainly with ground vehicles loading the aircraft. Some of those damages can be clearly recognised such as the one shown in Figure 1. However there are many damages which are hardly to be seen. A critical area among those is frames around the main cargo door of large aircraft such as the Boeing 747 where heavy loading trucks may collide with the lower frame and the locking mechanisms frequently. This has led to accumulated damage and resulted in some

Figure 1. Accidental damage in aircraft structures resulting from ground vehicles

cargo door lock failures in the early days of the Boeing 747 that triggered enhanced inspection of cargo door locks and has now become an issue for continuous monitoring. Aircraft do also have to withstand a variety of other types of repeating operational loads. One of them is hard landings where judgement of the hard landing is mainly referred to a pilot's – fairly subjective – judgement. Although landing gears are structures designed safe life and are hence replaced after defined intervals, it may be difficult to judge what effect the hard landing loads might have on a landing gear's adjacent structural components such as fittings, spars or frames to just name a few. Aircraft may however also be operated to their design limits which is specifically true with military aircraft. Figure 2 shows three examples in that regard a) a Panavia Tornado fighter aircraft, which has been initially designed in the late 1960ies for East-West attack in central Europe and is nowadays used for reconnaissance missions in countries such as Afghanistan and other places in the world, b) load spectra of a F-16 and CF-18 respectively, where the true operational spectrum has exceeded the design spectrum after a portion of its operational life. If those changes in load spectra would not have been monitored significant damage would have occurred to those types of aircraft and the air forces respectively. It has to be considered that a change in the operational conditions such as payloads, manoeuvres or environment will result in a higher amount of damage since the structure having been designed initially for specific operational conditions cannot be changed anymore. Besides metals carbon fibre reinforced polymers (CFRP) play an increasing role in aircraft structures nowadays where barely visible impact damage (BVID) is a source of significant concern and hence an option for monitoring.

Aircraft structures, specifically when it comes to commercial aircraft, are designed damage tolerant which allows structures to be designed lighter weight. Damage tolerance means that the structure considered is able to withstand damages up to a defined size above which a structure will then fail badly. Allowable damages in aircraft structures can achieve a significant amount in length ranging from a few millimetres up to even a metre or more in size, depending on where a crack is due to initiate. Figure 3 shows an example for a hidden corrosion along a front spar web that starts around the rivets at the inner side and gradually grows into two directions before it finally appears on the surface above the fillet seal. Assuming that a crack of 5 mm in length and more might be reliably detectable by an inspector the true crack length would already be in the order of centimetres or more when being finally detected.

Once damaged, a structure has to be repaired. Repairs in aircraft structures are standardised up to a certain degree. However there are many conditions where standardisation in repair does not apply such as with accidental damage. In those cases often tailored repair solutions have to be determined which might be monitored best continuously if technical conditions do allow. So far this has unfortunately not happened and in a few cases some major aircraft failed catastrophically from repairs such as with the Japan Airlines B-747 in 1985 or the China airlines B-747 in 2001.

Damage in aircraft structures can have a variety of reasons which have been summarised in Table 1 below. All of this damage is detected and quantified through non-destructive inspection (NDI) where most of the inspection is done on a visual inspection basis supported by NDI techniques such as ultrasonic and eddy current testing and is further supported by specific damage tolerance design criteria and/or loads monitoring if applicable at all. Inspection however requires a significant amount of effort specifically when the location to be inspected is located at a hidden place where a significant amount of components therefore has to be dismantled and reassembled again afterwards. This requires an aircraft to be out of operation for a substantial amount of time and it would be advantageous if this amount of time could be significantly reduced due to automation of the inspection process. Furthermore many of the subjective judgements done today by pilots such as with regard to hard landings could be made more objective through a loads monitoring system.

If structural health monitoring (SHM) is considered as the integration of sensors and possibly also actuators then the incident which triggered the birth of SHM in aeronautics has been the accidents of the de Havilland Comet aircraft in the early 1950ies (2). This aircraft as shown in Figure 4 below included the three significant engineering features of damage tolerant

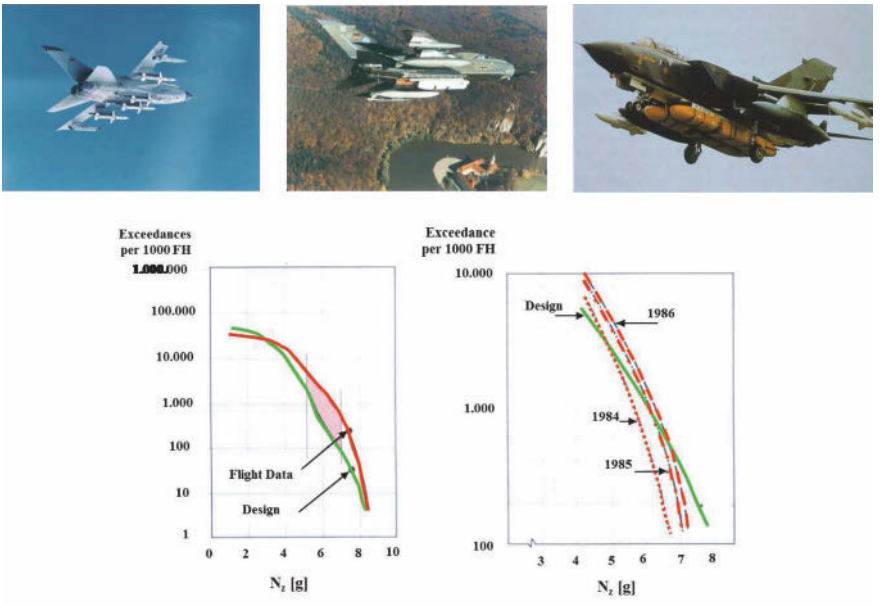

Figure 2. Changes in operational conditions of fighter airplanes of Panavia Tornado (top) and F-16 (bottom left) and CF-18 (bottom right) (1)

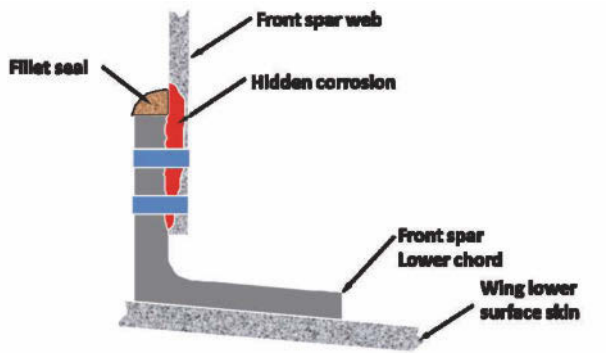

Figure 3. Wing front spar web with hidden corrosion of significant tolerable size

Issue	*Solution*	*Comment*
Accident	Visual and/or Non-Destructive Inspection (NDI); Repair	Barely visible damage can be overseen
Loads	Design spectrum; pilot judgement followed by possible NDI	Very subjective judgement
Fatigue & Fracture	Damage Tolerance Design; Major Structural Testing; NDI; Inspection Interval	Can be time consuming and labour intensive
Corrosion	Design; Corrosion Protection Plan; NDI; Inspection Interval	
Multi-Site Damage	NDI; Inspection Interval	
Repair	Quality Assurance; NDI; Inspection Interval	

Table 1. Issues of damage in aircraft structures and current means of solution

design, integrated jet engines and a pressurised fuselage as a novelty and has possibly been the most dramatic technology push which ever happened with an aircraft type in aviation history. However this technology push resulted in different significant aircraft crashes and hence losses within a very short period of time which triggered immediate measures to be taken on how to enhance aircraft safety in general. One of those measures taken has been the major airframe fatigue test (MAFT) which has nowadays become mandatory to be performed with regard to any new aircraft type going into operation. Figure 5 schematically shows such a type of test for an Airbus A300 and the Eurofighter Typhoon respectively. Along this test all operational loads are applied to the structure on ground with structural design to be validated with regard to its fatigue performance.

Another measure introduced also as a consequence of the Comet accident has been loads monitoring systems of the type shown in Figure 6. This system consists of eight accelerometers set at different trigger levels where each accelerometer measures the number the respective trigger level has been exceeded. Acceleration can be correlated with an aircraft's mass and is therefore a measure to characterise an aircraft's individual load and hence the load spectrum. The spectrum measured has then been a basis to determine a fatigue index FI which has been used to characterise an individual aircraft's usage and hence damage.

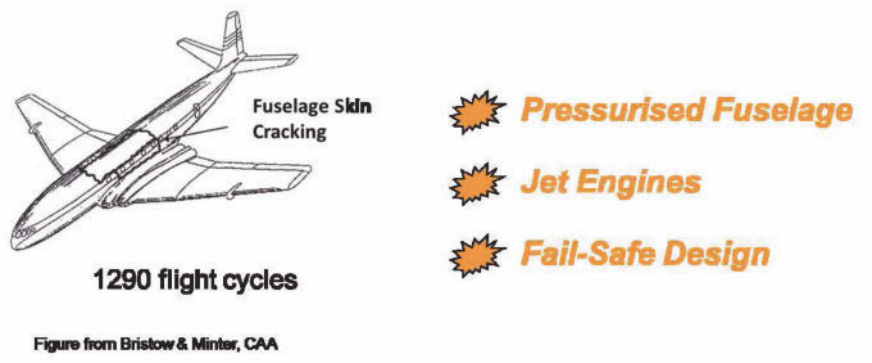

Figure 4. De Havilland Comet aircraft indicating the form of structural damage as well as the innovations made

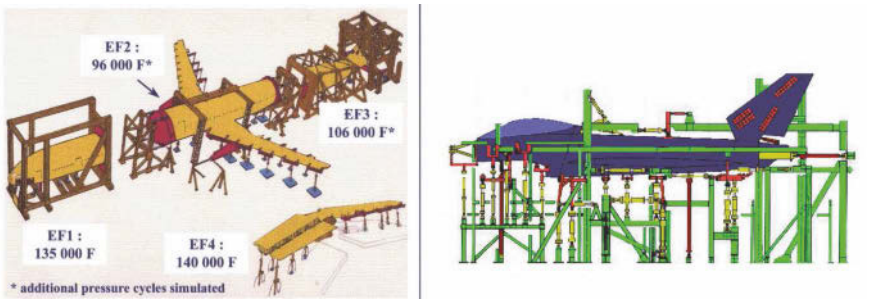

Figure 5. Major airframe fatigue tests performed on Airbus A300 (left) and Eurofighter Typhoon (right) (figures from H.-J. Schmidt/Airbus (left) and DASA (now Cassidian) (right))

Unluckily a trigger of many of the structural monitoring technologies introduced has been accidents. One of the milestones in that regard has been the Aloha Airlines Flight 243 accident in 1988 (Figure 7), where fracture of fuselage panels resulted from multi-site damage (MSD) along rivet lines due to ageing. This accident led to divide the life of aircraft structures into two phases. The first phase is conventionally around the first 15 years of an aircraft's life, where no specific measures have to be taken with regard to MSD and any measures with regard to ageing. It is only beyond this age where an aircraft is considered to age and an increasing in-depth analysis has to be done with regard to MSD and other issues of ageing resulting

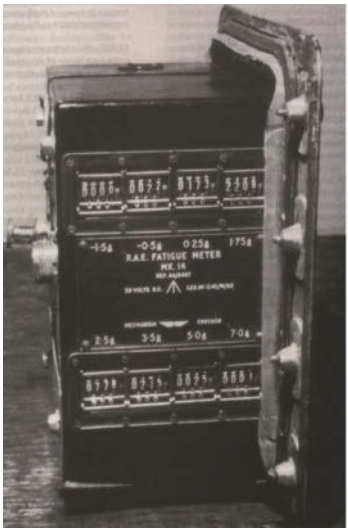

$$FatigueIndex(FI) = K_2 \times S_1 \times (2.31A + 0.03B + 0.001C + 0.001D + 0.28E + 3.43F + 10.36G + 18.63H + 1.16WL)$$

K_2 = Mission Coefficient
S_1 = Stores Configuration Coefficient
WL = Landing Coefficient
A bis H = Fatigue Meter Readings

Figure 6. Acceleration exceedance measurement system to be used for loads and fatigue monitoring in aircraft of the Royal Air Force since 1954 (3)

in an increased amount for inspection. It is also during this phase where damage monitoring and hence SHM becomes relevant.

Due to the fact that aircraft are designed damage tolerant and are therefore able to tolerate structural damage of significant size the amount of hull losses due to structural failure in aircraft has significantly decreased over the past decades, as shown in Figure 8. Today no more than 5% of the hull losses can be related to structural failure which is a consequence of enhanced structural understanding in terms of damage accumulation and a resulting effort in structural inspection. This inspection effort increases with an aircraft's increasing age and is hence a source for automation of the inspection process in case SHM can provide that option accordingly. Maintenance errors are a much higher source of error where SHM might be able to have a positive impact of alleviation too.

Implementing SHM into engineering structures in general requires the engineering structural design process to be understood. This has to include the operational loads to be applied on the respective structure. Those loads have to be assumed either in general when nothing else is known or have to be derived from past experience where they might have been measured on equivalent typed structures. Based on the structures' geometric shape

Figure 7. The Aloha Airlines Flight 243 accident as an impact to the ageing aircraft discussion

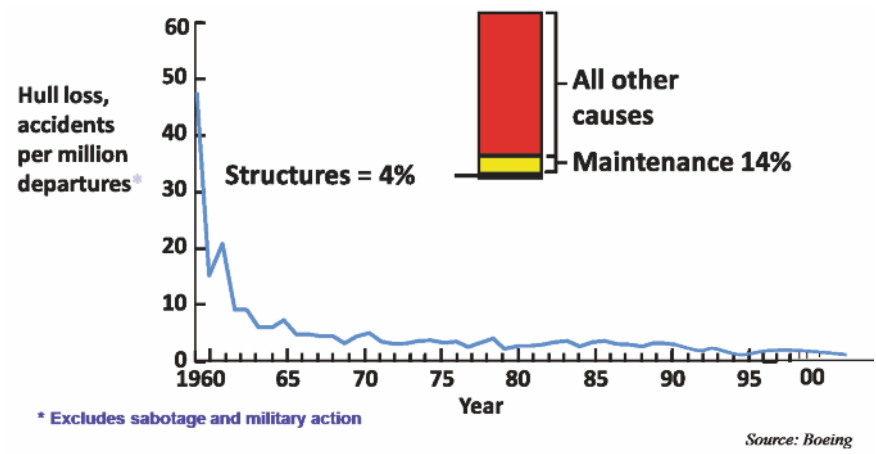

Figure 8. Jet fleet safety records and causes over the past 50 years

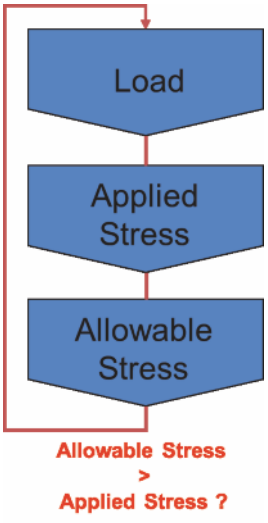

Figure 9. The structural design process

resulting in notches and the material chosen to build the structure itself, stresses and strains within the structure are calculated which results in the determination of local stresses and strains to be compared with the allowable stresses and strains resulting from the properties of the materials chosen. In case applied stresses are larger than allowable stresses a change in the geometric design might be required to reduce any stress concentration factors or a different material may have to be considered alternatively that would have to provide higher allowable stresses respectively.

A first parameter to be monitored in terms of SHM in that regard is therefore loads. The stress information obtained can then be used to evaluate fatigue damage in terms of a fatigue life evaluation and does allow locations on a structure to be determined where damage is most likely to occur. Those locations would then be the locations where damage monitoring may be performed best in terms of SHM. This approach in looking at loads monitoring first, combining this with structural assessment and finally performing damage monitoring at damage critical locations only is the most efficient way to minimise the number of sensors required in terms of SHM and which is therefore recommended to be pursued here. This approach is even applicable to multiaxial loading conditions.

Along this structural design process a central question arises with regard

to making a structure better available, lighter weight, more cost efficient and more reliable by making sensors and possibly actuators an integral part of the structure considered. What about looking at advanced sensors which are continuously becoming smaller, lighter and lower cost to become an integral part of a material and structure and further combining the sensors through advanced microelectronics and possibly wireless technology including advanced microprocessors and advanced signal processing? An answer to this question is SHM which is considered to be the integration of sensing and possibly also actuation devices to allow the loading and damaging conditions of a structure to be recorded, analysed, localised and predicted in a way that non-destructive testing becomes an integral part of the structure. SHM encompasses therefore of multitude of disciplines would those be structural strength including fatigue and fracture, structural dynamics, non-destructive testing, signal processing, and possibly much more.

What we therefore need to know to handle a structure adequately in terms of SHM is a structure's behaviour and performance which is described by the loads as well as the design and maintenance principles being applied. Depending on whether only loads or additionally also damage play a role, adequate sensors will have to be integrated which will have to work with appropriate assessment procedures would those be sensor signal processing as well as structural simulation tools. In that regard it is worth looking at a variety of emerging technologies where sensor and signal processing hardware as well as software and also manufacturing technologies that do allow for realisation of the SHM system have to be considered.

2 Loads and Overloads

Loads are the source of any material deterioration would this deterioration happen at the micro or at the macro scale. Loads are usually associated with mechanical loads where those are due to generate fatigue and fracture as damage. Loads may however also be environmental loads such as generated by temperature, humidity, irradiation or any other type of parameter that might lead to deterioration. Fatigue and resulting fracture is generated in a more complex way when loads are repetitive. Hence the time domain signal of a load needs to be known and therefore may have to be monitored. Since mechanical loads are usually the major point of concern in fatigue analysis considerations will be limited to mechanical loads here only. However ideas being expressed below may be synonymously transferred to other types of loads such as those being generated from environment. Loads are a fingerprint of a structure's operational conditions. Many of the different structural components therefore do not follow the same pattern of a load

sequence, specifically when they are exposed to a stochastic process and even combined with additional environmental loads. Only a very limited number of structures operate under a sequence of loads where the height of the load is permanently constant and where the spectrum will be called 'constant amplitude'. Most of the loads sequences have their specific spectra. Just imagine an aircraft and the load at the wing attachment box as shown schematically in Figure 10. While the aircraft is on the ground the load might be slightly compressive or close to zero while once the aircraft has taken off the load increases significantly to a high tensile load being directly related to the aircraft's flight load. This load cycle is also called the ground-to-air cycle. While in the air, the aircraft will manoeuvre and face different gusts which will result in dynamic loads cycling around the mean load carrying the aircraft. Once the aircraft lands again the tensile load will vanish or even turn into compressive. Different other applications will show different time domain loading patterns where a few examples are provided in Figure 11.

Reasons for a load-time function may be various and the result of a superposition of different effects as shown schematically in Figure 12. Besides a main load being composed of the structure's weight and a potential payload which can be both mainly considered to be static there are additional loads being generally of a fatigue load nature with manoeuvre loads usually occurring at lower frequencies when compared to higher frequency loads being generated from vibrations.

Load sequences themselves are difficult to be characterised from a time domain point of view such as shown in Figure 11. Different load cycle counting procedures have been developed during the 1930ies to 1970ies where the rainflow cycle counting method (5) has turned out to be the recently most widely accepted. Figure 13 shows a time-domain sequence with its various peaks and troughs where the shape of the time-domain signal can be imagined as the bottom of a water basin reservoir. Now imagine this reservoir to be filled to its top with water (Figure 13 left) and we are gradually shaving the bottom of the water basin from its lowest trough upwards. The first trough which will be hit will be load level -2. Once cut water will flow out from an upper level of +4.5 down to a lower level of -2. This is considered as the cycle of the largest loading span and has been registered as cycle 3 in the table shown in the upper right of Figure 13. The next trough to be hit is at load level -1.5 where water will flow out from load level 3.5 down to -1.5 and is considered as cycle 1 in the table in Figure 13. This is followed then by the trough at load level -1 where water now only flows out from load level 2.5 down to -1 because water level was already reduced from 4.5 to 2.5 due to load cycle 3. Finally a trough at load level +1 is hit where

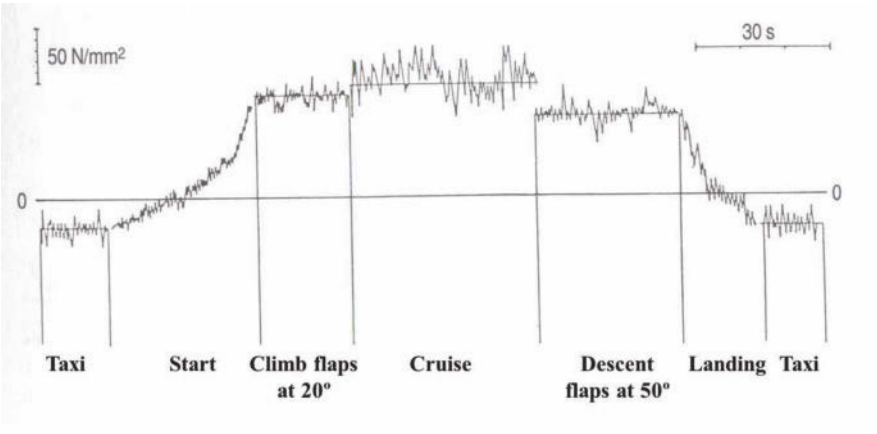

Figure 10. Stress Sequence in Tension Girder of the Wing Root of a Transport Aircraft (4)

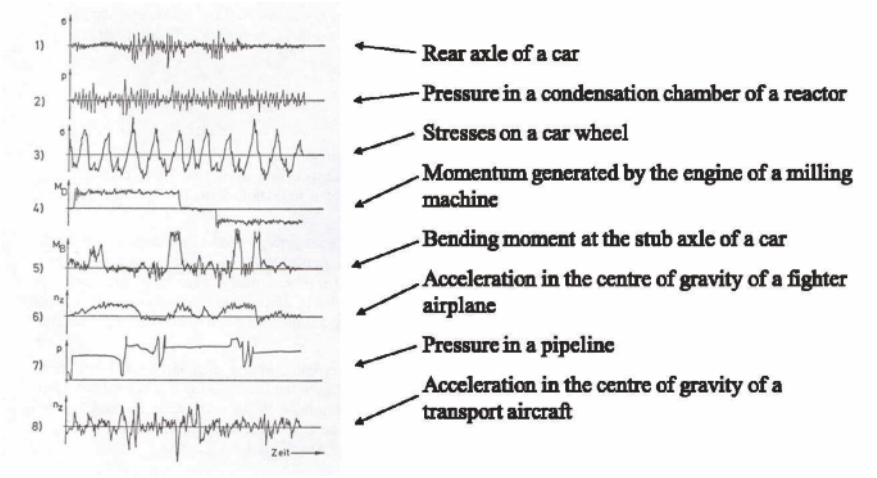

Figure 11. Examples of load sequences for different structures and systems (Figure from (4))

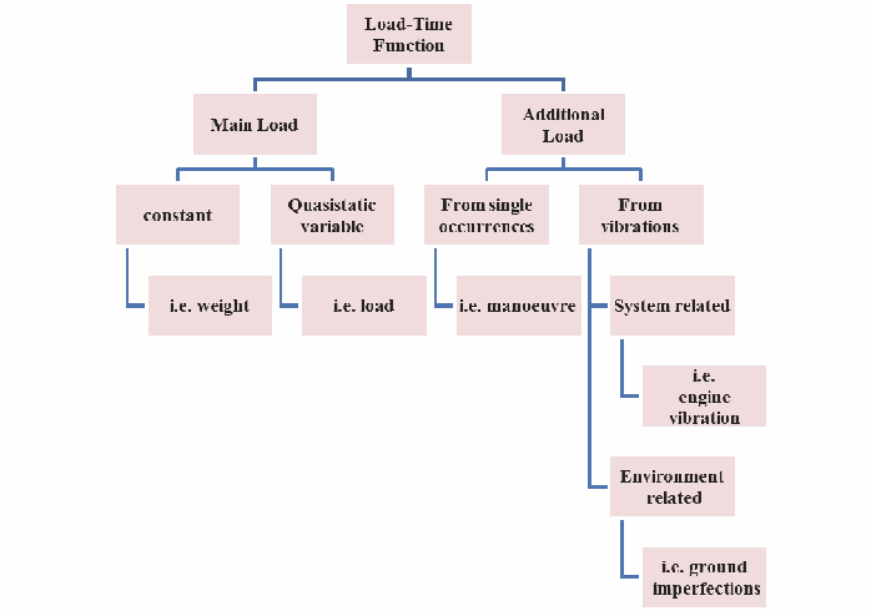

Figure 12. Reasons for load-time functions

water drops from load level 2.5 down to 1 due to the water level reduction already resulting from cycle 1. There is a residual remaining with a trough a load level +2 which cannot be considered since it is unknown where the load sequence is going to continue. With conventional load sequences and their generally large number of cycles this residual can be considered to be negligible. Each cycle can now be represented either in terms of the maximum and minimum load/stress or the amplitude and the mean as shown in the table in Figure 13. The cycles can be further plotted in terms of their loading range as exceedances as shown on the lower left of Figure 13. The shape of this plot can be also considered as a characteristic of a spectrum. Just imagine the spectrum would be constant amplitude. In that case the spectrum would turn out to be of squared shape as shown schematically in Figure 14. Every spectrum being of a random service load nature would turn out to be of a non-squared shape when all spectra are normalised on the same maximum load. In that case the smaller area the spectrum shape covers the weaker the spectrum is considered to be in terms of damaging.

Load spectra may be a combination of different discrete events and this at different levels. Assume an aircraft performing a series of different flights.

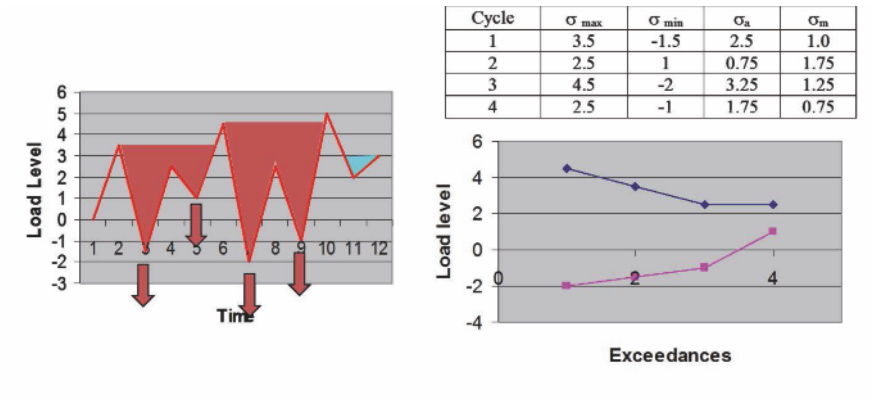

Cycle	σ_{max}	σ_{min}	σ_a	σ_m
1	3.5	-1.5	2.5	1.0
2	2.5	1	0.75	1.75
3	4.5	-2	3.25	1.25
4	2.5	-1	1.75	0.75

Figure 13. Rainflow cycle counting method (5)

Each flight consists of a variety of different load cycles where the ground to air cycle might be the dominant one added by a variety of smaller load cycles being characterised by flight manoeuvres as well as gusts. Load spectra for civil aircraft may be of a mainly linear shape nature in accordance to the examples provided in Figure 14. Each flight again may be of a different characteristic. Most of the flights are of a smooth character with a lower maximum load. However there is also a limited number of flights under turbulent conditions where loads may be more severe and occasionally an aircraft might even have to fly through a thunderstorm where the maximum load might even be higher. Flight spectra have been characterised and as a consequence standardised for a variety of applications where some examples of a mainly aeronautical nature can be found in (6). One of the most popular aeronautical load spectra is the Transport WIng Standard (TWIST) (7) shown in Figure 15. The spectrum consists of principally two sub spectra being a flight spectrum and a ground taxiing spectrum respectively. The ground taxiing spectrum is again divided into two steps (load levels) while the flight spectrum is divided into ten steps, with both resulting in a mainly linear shaped spectrum.

Detailed numbers for the TWIST spectrum are provided in Table 2. Besides being divided into the load steps I to X there is also a division into flight types A to J, where flight type A represents the most severe flight type with the highest loads and the lowest likelihood to occur during an aircraft's operational life while flight type J is the flight type to occur most and consisting of the lowest loads distribution.

Load cycles as described for the TWIST spectrum in Table 2 may also

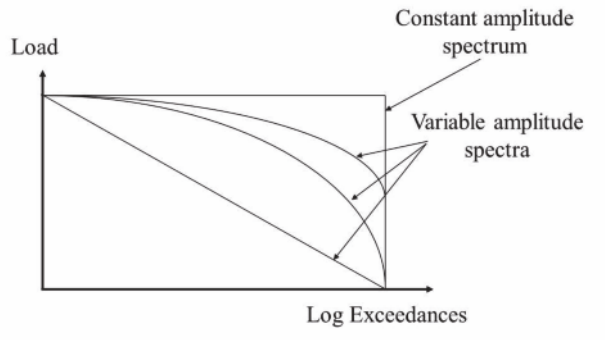

Figure 14. Shape of different loading spectra

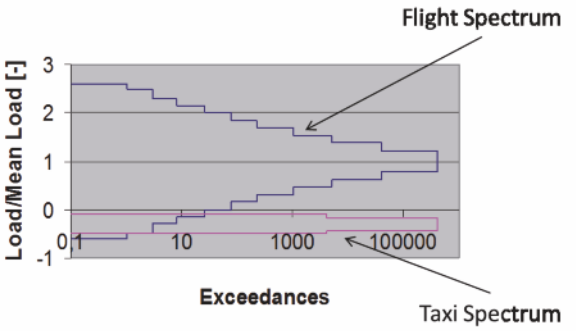

Figure 15. Transport Wing Standard (TWIST) spectrum (7)

Flight type	Number of Flights	Cycles per step										Cycles per flight
		I	II	III	IV	V	VI	VII	VIII	IX	X	
A	1	1	1	1	4	8	18	64	112	391	900	1500
B	1		1	1	2	5	11	39	76	366	899	1400
C	3			1	1	2	7	22	61	277	879	1250
D	9				1	1	2	14	44	208	680	950
E	24					1	1	6	24	165	603	800
F	60						1	3	19	115	512	650
G	181							1	7	70	412	490
H	420								1	16	233	250
I	1090									1	69	70
J	2211										25	25
Total cycles in all		1	2	5	18	52	152	800	4170	34800	358665	
Exceedances		1	3	8	26	78	230	1030	5200	40000	398665	

Table 2. Defined load spectra descriptors of the TWIST spectrum (7)

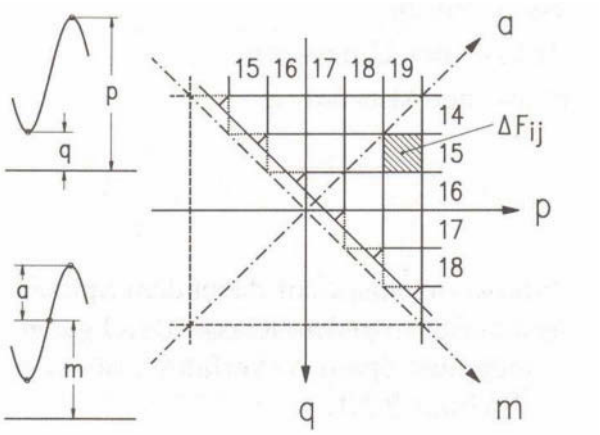

Figure 16. Load matrix descriptions and definitions (figure from (4))

be summarised and described in a matrix as the number of load half cycles going from a minimum load level q (trough) to a maximum load level p (peak) within a complete load spectrum determined in accordance to the rainflow cycle counting method mentioned before. Numbers 14 to 19 indicated as an example in Figure 16 represent arbitrary load levels which have to be decided upon in accordance to the specific needs. In the case of the TWIST load sequence the total number of load levels is 10. Figure 16 hence represents a matrix where each of the elements ΔF_{ij} represents the number of cycles going from load class i to load class j. Going along the horizontal axis and looking at the upper right triangle provides all the peaks p with increasing number while looking at the vertical axis downwards and the matrix's lower left triangle provides all the troughs q respectively. Similar considerations can be made with amplitudes a and means m when converting those as follows:

$$\begin{array}{rclrcl} q & = & m-a & p & = & m+a \\ a & = & (p-q)/2 & m & = & (p+q)/2 \end{array}$$

A rainflow matrix as shown in Figure 16 and having been once filled can be pseudo-randomised in accordance to a procedure described in Figure 17. The 32x32 rainflow matrix shown in Figure 17 is filled with numbers a_{ij}. Assume the randomised service load sequence to originate from class α. In this case a term T_α is determined in accordance to $T_\alpha = \sum_{j=\alpha+1}^{n} a_{\alpha j}$ with

a random number R_n being determined as:

$$R_n = A \cdot R_{n-1} + (B + 1 + W)\,(MOD\,M)$$

With $M = 2^r$ and $r = 1 + INT\,(\ln T_\alpha / \ln 2)$

$$\begin{aligned} D &= M - T_\alpha \\ A &= (5)\,MAX\,(M/2 - 3) \\ B &= (3)\,MAX\,(M/4 - 1) \end{aligned}$$

$W = +1$ when towards a peak and $W = -1$ when towards a trough.

For the very first cycle when loading turns towards a peak R_{0i} turns out to be:

$$R_{01} = D_i + \sum_{j=i+1}^{16} a_{ij} \text{ for } i = 1...15 \text{ and } R_{0i} = D_i \text{ for } R_{0i} = D_i \text{ for } i = 16...32$$

When the first cycle turns towards a trough R_{0i} is determined as:

$$R_{0i} = D_i \text{ for } i = 1 \,...\, 17 \text{ and } R_{0i} = D_i + \sum_{j=17}^{i=1} a_{ij} \text{ for } i = 18 \,...\, 32.$$

Target load level β is achieved when $R_n - \sum_{j=\alpha+1}^{\beta} a_{\alpha j} \leq 0$ and $a_{\alpha\beta}$ is now reduced by 1.

If load level β is a peak (as shown in Figure 17) the same procedure is determined the opposite way to determine load level γ as shown in Figure 17. This procedure is then continued until all peaks and troughs within the matrix have been absorbed. A resulting load sequence determined might then look like the one shown as an example in Figure 18 where N_0/N_1 is the ratio of the number of cycles of zero crossings versus the complete number of cycles within the load spectrum.

3 Fatigue, Fracture and Damage Tolerance

3.1 Fatigue

Fatigue and fracture do specifically occur in areas where stresses and strains concentrate. Locations of stress and strain concentrations are notches where stresses and strains do increase significantly by even a factor. Figure 19 left shows such an example for an elliptic notch where the following equation

$$(\sigma_\varphi)_{\max} = S\left(1 + 2\frac{1+c}{1-c}\right) = S\left(1 + 2\frac{a}{b}\right) = S\left(1 + 2\sqrt{\frac{a}{\rho}}\right) \qquad (1)$$

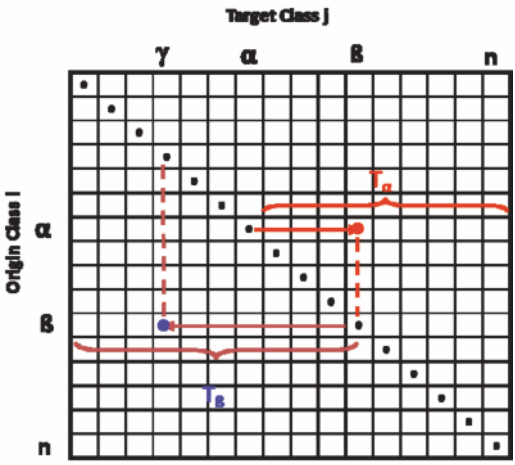

Figure 17. Pseudo-random load sequence generation scheme based on a rainflow matrix (8)

Figure 18. Pseudo-random load sequence generated from a rainflow matrix

does allow the maximum stress in the notch root $(\sigma_\varphi)_{\max}$ to be determined as a function of the nominal stress S, the notch depth a and the notch root radius ρ as shown in Figure 19.

Nominal stress S resulting from an axial load F is usually defined as $S = F/A$ where A is the cross net-section. Similar definitions can be made for bending and torque. It is important that one continuously sticks to the same nominal stress definition. Stress increase due to a notch is defined as

$$K_t = \frac{(\sigma_\varphi)_{\max}}{S} = \frac{\text{maximum stress}}{\text{nominal stress}}$$

where K_t is named the stress concentration factor. K_t is derived from a component's pure elastic behaviour and its definition is therefore only

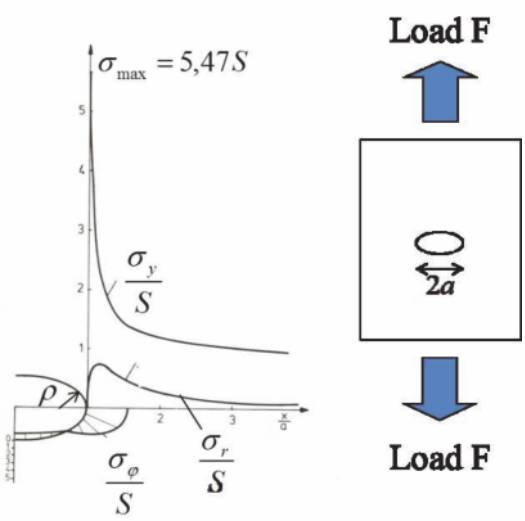

Figure 19. Stress concentration in a notch root

valid when loading is macroscopically elastic with small scale yielding in the notch root being allowed only. The definition is also just valid for one type of loading would this either be tension, bending or torsion. A different type of loading will also result in a different K_t value. K_t values can be either determined from handbooks (i.e. (9)) or might have to be determined through a FE analysis.

To characterise the fatigue behaviour of an unnotched (material) or a notched component (structure) constant amplitude fatigue tests are performed at different load levels as shown in Figure 20. The result obtained is a fatigue life curve (S-N curve) for either crack initiation or complete fracture. Those S-N curves can be linearized when being plotted in a log-log scale, where an endurance limit can be seen at fatigue lives around 10^6 cycles, resulting in a bi-linear relationship in a log-log scale in the end. An S-N curve does depend upon the material, component (geometry/shape), loading and nominal stress definition considered. S-N curves may be determined experimentally or may be taken from handbooks (i.e. (10)).

Once an S-N curve is made available fatigue life of a structure can be estimated. The way such an estimation is done in principle is shown as an example in Figure 21. Assume a load sequence to consist of the following

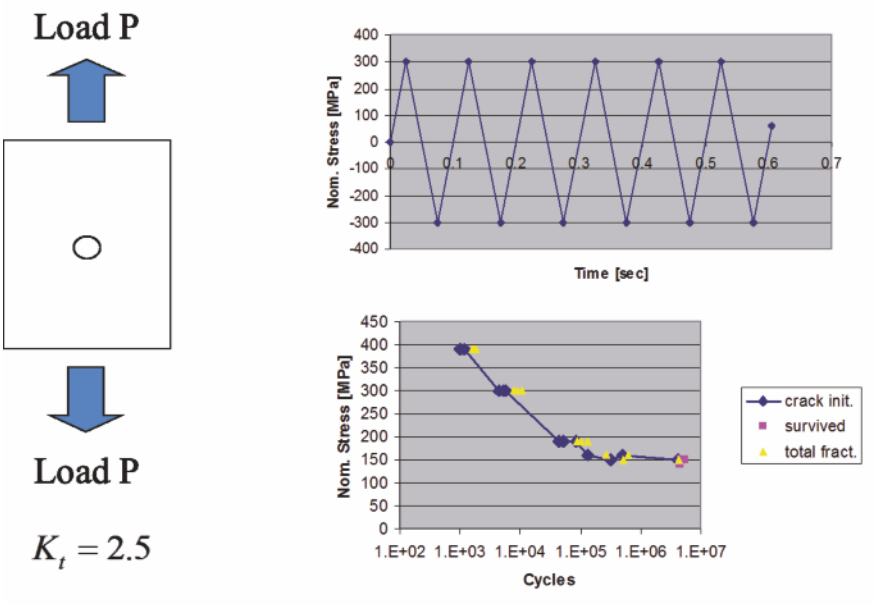

Figure 20. Determination of a constant amplitude S-N curve of a notched specimen

three loading blocks: a) $n_1 = 6$ cycles of a maximum stress of 300 MPa, b) $n_2 = 4$ cycles of a maximum stress of 400 MPa and c) $n_3 = 5$ cycles of a maximum stress of 200 MPa. For the stress range block a) the component would endure around $N_1 = 2 \times 10^5$ cycles, which would result in a linearized damage D_i per load cycle to be $D_i = 1/N_1$ or for the complete block $D_1 = n_1/N_1$. The same is applied for blocks b) and c) where N_3 turns out to be infinite in the case of block c) and hence damage per loading cycle results in being zero. Damage is assumed to accumulate linear in accordance to the Palmgren-Miner [11,12] rule which is defined as shown in Figure 21. Fatigue life is achieved when accumulated damage D turns out to be unity.

With such an approach combined with a FE-analysis accumulated fatigue damage can be virtually calculated for each element allowing areas of high damage accumulation to be determined. These areas are those where damage monitoring then will have to occur first. It therefore turns out that this way of fatigue life evaluation is an essential strategic means for an efficient SHM process. What that means in terms of a SHM strategy can be summarised as follows:

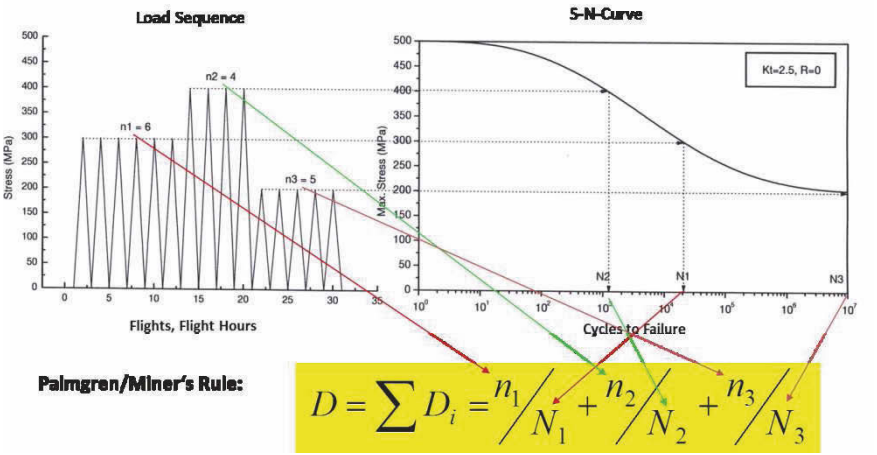

Figure 21. Fatigue life evaluation according to Palmgren Miner's rule

1. Establish a loads monitoring system based on load sequence measurement that allows the operational loads sequence to be monitored, analysed and stored as a rainflow matrix.
2. Use the rainflow spectrum to perform fatigue life evaluation under true service loading conditions and determine the locations on the component considered where damage is most likely to occur (hot spots).
3. Equip hot spots with damage monitoring systems that will possibly allow the initiation of a crack to be detected but will certainly detect an allowable damage such as a defined crack length in accordance to the damage tolerance principle.

3.2 Fracture and Damage Tolerance

Structures when being loaded can withstand a considerable number of load cycles until they fracture. Fracture is considered as a damage condition defined which might be a crack of a defined size. When a component of a material, shape and manufacturing process being well defined is fatigue loaded it will fracture at a specific number of fatigue cycles. If the test is done again on a next component made of the same material, shape and manufacturing process it will most likely fail at a different number of fatigue cycles. Further repetitions of the fatigue test will finally result in a scatter band of fatigue lives as shown as an example in Figure 22. Looking at the resulting S-N curve this does result in a zone where: a) nothing fractures, b) fracture occurs and c) everything has fractured. If a structure is to be

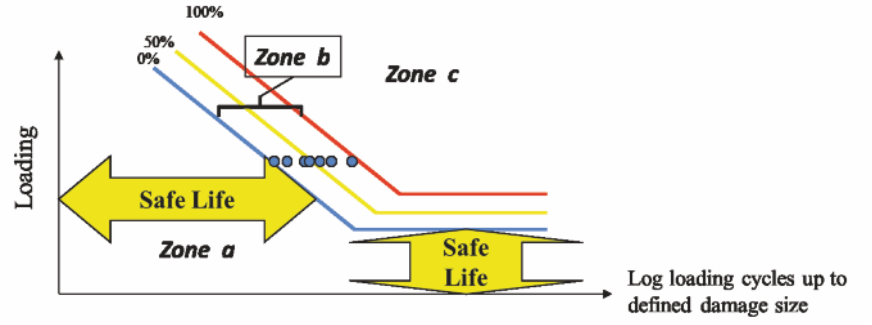

Figure 22. Scatter in S-N curves and the impact on structural design principles

designed such that it is not allowed to fracture it has to be designed such that it falls into zone a). Once the component has achieved the fatigue life defined by the S-N curve of 0% of probability of fracture the component will have to be removed although it might still have a substantial amount of remaining fatigue life. This is what is called *safe life design*. Since the abscissa of an S-N curve is plotted in a logarithmic scale the scatter band of fatigue lives (zone b)) may easily be in the range of a factor of two and more. Hence if the component mentioned before having been removed under safe life design conditions would be run until its true fracture life it might have lasted an additional number of fatigue cycles possibly of the same amount as it would have lasted under safe life design. Allowing a component to be run up to fracture however requires damage mechanisms within the component to be understood and the component to be inspected at well-defined intervals. This is what is called *damage tolerant design* and where SHM comes into play. Damage tolerant design allows a structure to last longer or if this is not desired to apply higher stresses which results in lighter weight design. The latter is what aeronautics has specifically taken advantage of and what now has become standard specifically in the commercial aviation world.

The idea of damage tolerant design can also be extended to engineering structures in general. In that case a component in a structure may fail as long as neighbouring components may be able to take over the loads in the sense of a redundancy and the structure with the resulting fracture may be even controllable under these circumstances. This is what is also generally known as *fail safe design*. Figure 23 shows the range damage tolerance can have within potential fatigue life. If microcracking is not considered

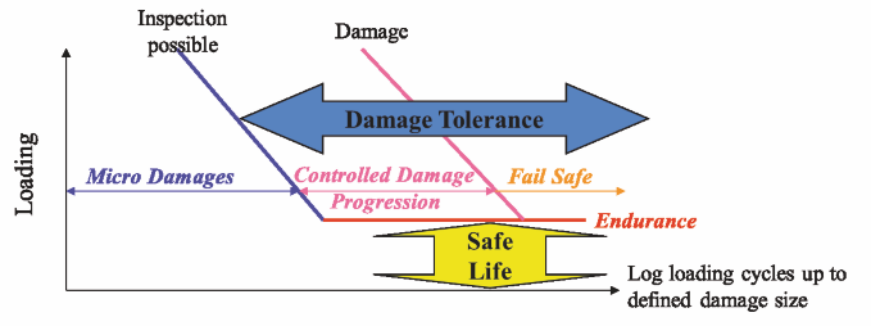

Figure 23. Range of damage tolerance along structural fatigue life

to impair the structure's integrity, damage tolerance starts from where a crack can be reliably observed and damage progression can be controlled until a tolerable damage constellation within the fail safe area with the size of tolerable damage being defined by structural design. A further aspect to be considered is that non-destructive testing concepts have to be further developed along the design phase of a damage tolerant structure (13).

A key issue within damage tolerant design is the knowledge on how cracks propagate. From a very generic principle cracks can even be considered as a notch for which Eq. (1) might be applicable and where the notch depth a may be equivalent to the crack length and hence large when compared to the notch radius ρ being extremely small in a crack leading finally to an incredibly high stress concentration. This would however only be true with a brittle material where material and structural conditions are fully elastic. With ductile materials crack tips however become blunt due to plasticity which then significantly changes the stress intensity and makes Eq. (1) to become invalid in that case.

Cracks can be principally loaded under the three different conditions shown in Figure 24 and which are called the cracking modes or modes simply. Mode 1 represents an axial tensile loading, mode 2 a bending loading and mode 3 a twist loading respectively. Along the following only cases of mode 1 will be considered.

Stresses σ_{kl} around the tip of an arbitrary crack under arbitrary loading can be principally determined on the basis of the following equation:

$$\sigma_{kl} = \frac{1}{\sqrt{2\pi r}} \left[\underbrace{K_I f_{kl}^{I}(\varphi)}_{\text{Mode I}} + \underbrace{K_{II} f_{kl}^{II}(\varphi)}_{\text{Mode II}} + \underbrace{K_{III} f_{kl}^{III}(\varphi)}_{\text{Mode III}} \right] \qquad (2)$$
$$k, l = x, y, z$$

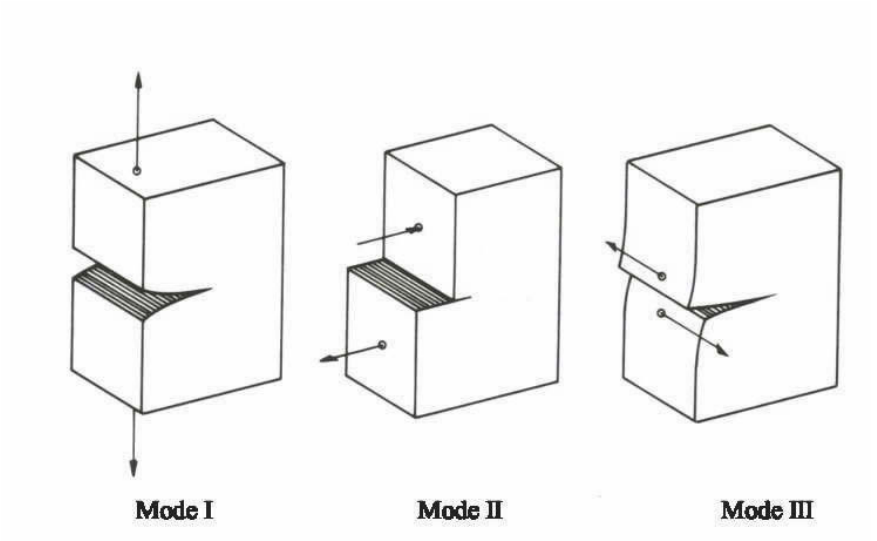

Figure 24. Different modes of fracture

where r is the radius from the centre of the coordinate system as shown in Figure 25 for a crack in an infinite plate under bi-axial loading, K_I , K_{II} and K_{III} are the stress intensities for the different modes and $f(\varphi)$ are dimensionless functions depending on the crack mode. In the case of mode 1 K_I turns out to be:

$$K_I = \sigma\sqrt{\pi a} \quad \left[N\Big/\sqrt{mm^3}\right] \tag{3}$$

Since the geometry of the component has an influence on the stress intensity factor Ka geometry factor $Y$is additionally introduced extending Eq. (3) to become

$$K_I = Y\sigma\sqrt{\pi a} \quad \left[N\Big/\sqrt{mm^3}\right] \tag{4}$$

Reference for all geometry factors is a crack in an infinite plate where Y is unity while for all others this will differ, for which an example is given in Figure 26 for a finite plate cracked. Further geometry factors can be found in handbooks such as [14-17] and possibly also in other relevant publications or may have to be determined by numerical means.

When a component is fatigue loaded the load alternates between a minimum and a maximum load and hence stress. The stress intensity factor

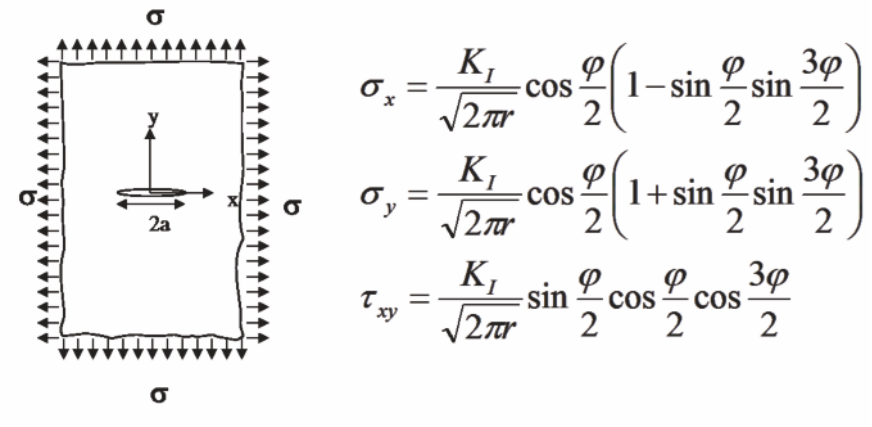

$$\sigma_x = \frac{K_I}{\sqrt{2\pi r}} \cos\frac{\varphi}{2}\left(1 - \sin\frac{\varphi}{2}\sin\frac{3\varphi}{2}\right)$$

$$\sigma_y = \frac{K_I}{\sqrt{2\pi r}} \cos\frac{\varphi}{2}\left(1 + \sin\frac{\varphi}{2}\sin\frac{3\varphi}{2}\right)$$

$$\tau_{xy} = \frac{K_I}{\sqrt{2\pi r}} \sin\frac{\varphi}{2}\cos\frac{\varphi}{2}\cos\frac{3\varphi}{2}$$

Figure 25. Stresses under mode 1 around a crack tip for a crack in an infinite plate under bi-axial loading

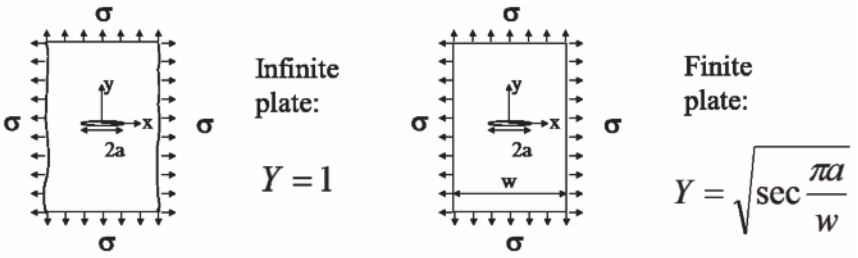

Figure 26. Geometry factors Y for a cracked infinite and finite plate

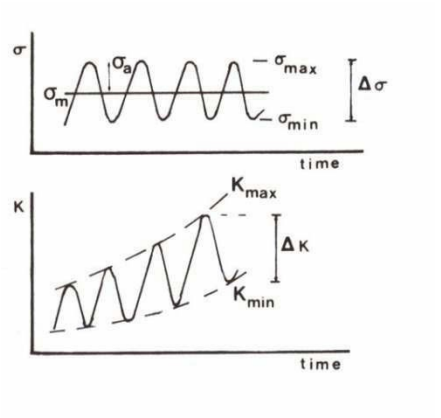

Figure 27. Development of stress intensity for a crack under fatigue loading

K being dependent on stress will therefore alternate as well and can therefore be differentiated between a minimum and a maximum value as to the following:

$$\begin{aligned} K_{\min} &= Y\sigma_{\min}\sqrt{\pi a} \\ K_{\max} &= Y\sigma_{\max}\sqrt{\pi a} \end{aligned} \tag{5}$$

and with a range ΔK being

$$\Delta K = K_{\max} - K_{\min} = Y\left(\sigma_{\max} - \sigma_{\min}\right)\sqrt{\pi a} \tag{6}$$

Since K also depends on the crack length and the influence of the crack length might be less under the minimum load than under the maximum load due to an effect being called crack closure, development of crack intensities along a fatigue test may develop as schematically shown in Figure 27.

What can be indirectly observed from the lower plot in Figure 27 is the nonlinear propagation of a crack length a over fatigue life. When a fatigue test is performed on a cracked plate under constant amplitude loading crack propagation can be observed as to the right hand curve of the left diagram in Figure 28. A similar test done at a higher load level will allow the crack to propagate at higher speed and hence result in the left hand curve of the left diagram in Figure 28. When plotting the change in crack propagation over fatigue life da/dN over the range in stress intensity ΔK in a logarithmic scale, a fairly linear relationship is obtained as can be seen from the right

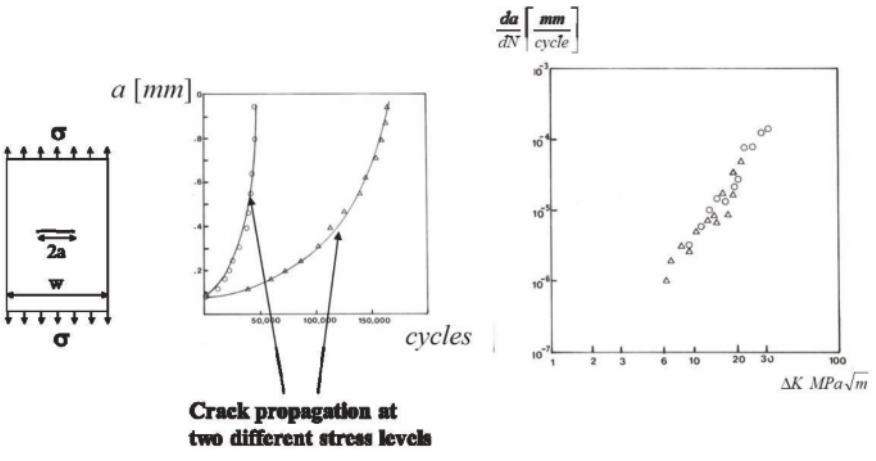

Figure 28. Crack propagation behaviour under two different stress levels

hand diagram on Figure 28. This relationship described as

$$\frac{da}{dN} = C_P \left(\Delta K\right)^{m_P} \tag{7}$$

has been determined by Paris (18). It has to be mentioned that constants within Eq. (7) are only valid for a specific stress ratio $R = \sigma_{\min}/\sigma_{\max}$ (or strain ratio in case of strain control) and need to be re-determined in case R changes. Furthermore crack propagation rate goes to infinity once it reaches fracture toughness, where stress intensity is expressed in terms of K_c. Forman (19) therefore extended the Paris equation to become

$$\frac{da}{dN} = C_F \frac{\Delta K^{m_F}}{\left(1-R\right) K_c - \Delta K} \tag{8}$$

Crack propagation calculations and hence estimations can now be made loading cycle by loading cycle in accordance to the following steps:

1. Assume an initial crack length a_0 that can be reliably detected by means of non-destructive testing or SHM;
2. Determine the geometry factor Y either from handbooks, literature or by numerical analysis;
3. Determine the nominal stress from the maximum or minimum load to be applied within the load cycle considered;

4. Calculate the minimum and maximum stress intensity factors $K_{\min}$ and $K_{\max}$ as well as resulting ΔK;
5. Calculate crack propagation rate da/dN and hence crack extension Δa for the load cycle considered;
6. Add crack extension Δa to the initial crack length a_0 to determine the new crack length a to be used as the initial crack length in step 1 for the next load cycle;
7. Continue with step 2 accordingly.

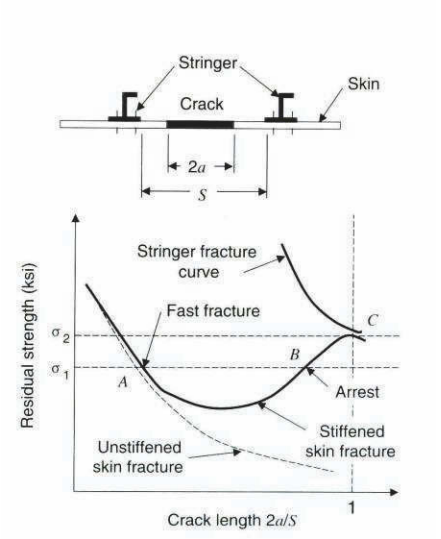

Figure 29. Influence of stiffeners along a damage tolerant structural design (source: (20))

That crack propagation calculation is a necessity within damage tolerance considerations can be seen from the examples provided in Figures 29 and 30 respectively. Residual strength of a cracked structure follows a hyperbolic curve in case strength is plotted over crack length and the crack is considered to propagate in an infinite environment. However if a crack stopper or at least retarder is in the crack progression's way such as a stringer in an aircraft structural component then residual strength of a crack in such a stiffened panel is again reduced such as shown schematically in Figure 29. On the other hand the stiffening stringer has a residual strength curve too which has to be significantly above the one for the panel such that a crack

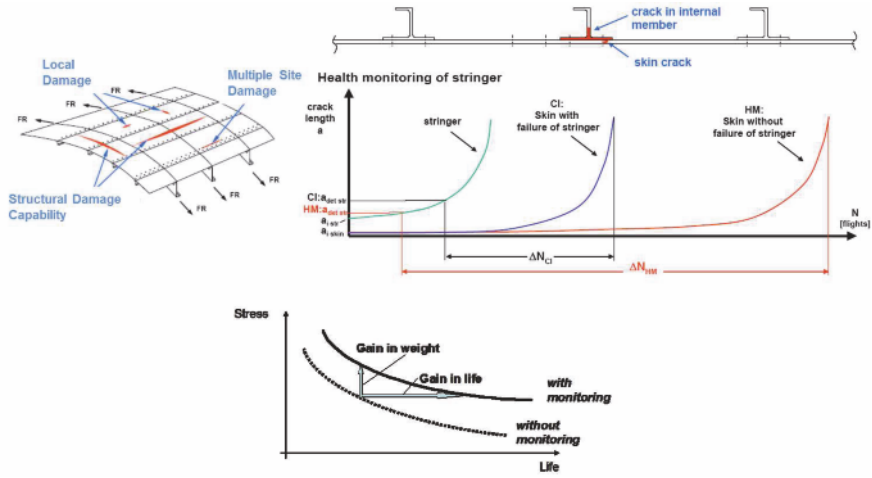

Figure 30. Gain in structural life through health monitoring (HM) of a stringer in an aircraft panel when compared to conventional inspection (CI) (Source: H-J Schmidt, Airbus)

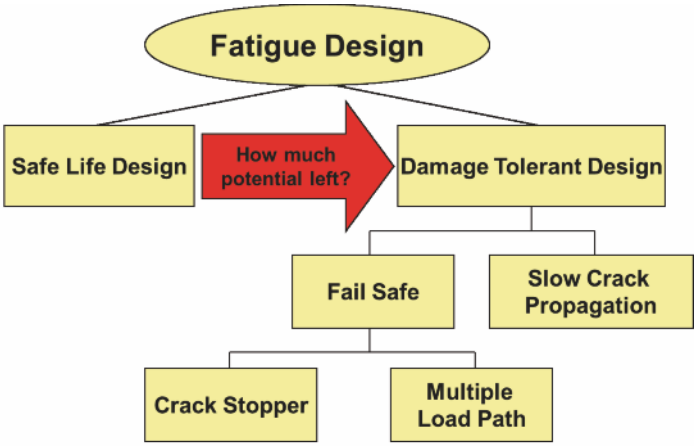

Figure 31. Transition from safe life to damage tolerant design

not having been detected in the panel will not exceed a critical size in case the structure would experience the maximum load along the given design spectrum. Furthermore an initial crack size has to be detected reliably. Only under those circumstances a crack propagation life can be calculated and a resulting inspection period defined. However if a component cannot be inspected, assumptions have to be made with regard to its crack propagation life where crack propagation estimates will have to be on the safe side. Assume an aircraft fuselage component of the type shown in Figure 30 and the condition that frames and stringers might not be inspectable, hence the structure can only be inspected from the aircraft's outer side. Under those conditions frames and stringers have to be considered broken in case crack propagation life and hence the inspection interval has to be based on crack propagation observed on the fuselage's outer surface only. However if stringers and frames were inspectable such as with an SHM system then assumptions for crack propagation could be changed leading to a significant increase in crack propagation life determined or inspection interval defined. If this increase in fatigue life would not be of interest for the case considered then another option would be to increase stresses applied which would then lead to a decrease in structural material to be used and hence result in lighter weight design which again is identical to the effect already observed with damage tolerant design. Implementing SHM is therefore in many cases nothing else than enhancing the idea of damage tolerant design or in other words determining how much potential a structure has in accordance to the damage tolerance principle shown in Figure 31. That damage tolerance has a significant impact on current aircraft structural design can be seen from Figure 32 where areas where crack growth (C.G.) is the relevant design parameter have been clearly marked. Those areas have to be inspected in well-defined intervals where the interval is defined by the metallic material considered, the component's shape, the loading condition including the sequence, an initial detectable crack and a final allowable crack.

Size of the initial detectable crack again depends on a variety of parameters such as the non-destructive testing (NDT) means used as well as the location of the crack to initiate. Figure 33 provides an overview of NDT techniques traditionally used in aeronautics and the possible sensitivities to be achieved. In that context it has to be kept in mind that more than 90% of an aircraft's structure is inspected by visual means and that only a very limited number of critical components is inspected by techniques such as ultrasonics, eddy current or radiography. What is important in that regard is that the probability of detection (POD) of the damage (i.e. crack) considered has to be > 95 % hence the initial crack assumed has to be larger than what the NDT method applied may be virtually able to detect in average.

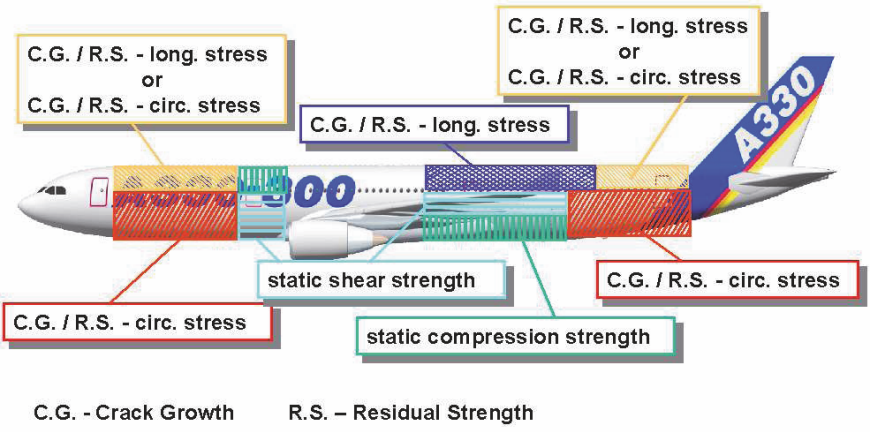

Figure 32. Critical design parameters along an aircraft fuselage (Source H-J Schmidt, Airbus)

NDT METHOD	MINIMUM DETECTABLE CRACK LENGTH	HIGH PROBABILITY DETECTABLE CRACK LENGTH (> 95%)	QUALIFYING REMARKS
X-Ray (XR)	4 mm	10 mm	Dependent on structure configuration, thickness and geometry. Detectable values increase considerably over 12 mm thickness.
Ultrasonic (US)	2 mm	5 mm - Outer fuselage skins 6.5 mm - Inner fuselage skins 2-6 mm – Forgings, spars, extrusions, etc.	Cracks from fasteners holes with fasteners in place Dependent on structure geometry and material type
High frequency Eddy current (HF/EC)	2 mm (surface) 0.5 mm (bore holes)	2.5 mm – Surface 1.0 mm – Bore holes	Surface cracks in accessible areas Bore holes with fasteners removed, using rotating probes
Low frequency Eddy current (LF/EC)	2 mm	4.5 mm – Outer fuselage skins 8 mm – Inner fuselage skins	Cracks from fastener holes with fasteners in place. For thicker structures, the detectable length is approximately equal to the thickness up to 5 mm. Between 5 mm and up to a maximum of 12 mm the detectable length is approximately equal to 2x the thickness. Above 12 mm detection cannot be guaranteed.
Magnetic particle (MP)	2 mm	4 mm Surface	Surface breaking – component removed from aircraft
Liquid penetrant (LP)	2 mm	10 mm Surface	Surface breaking – dependent on surface condition

Figure 33. Detectable crack length for different popular NDT techniques

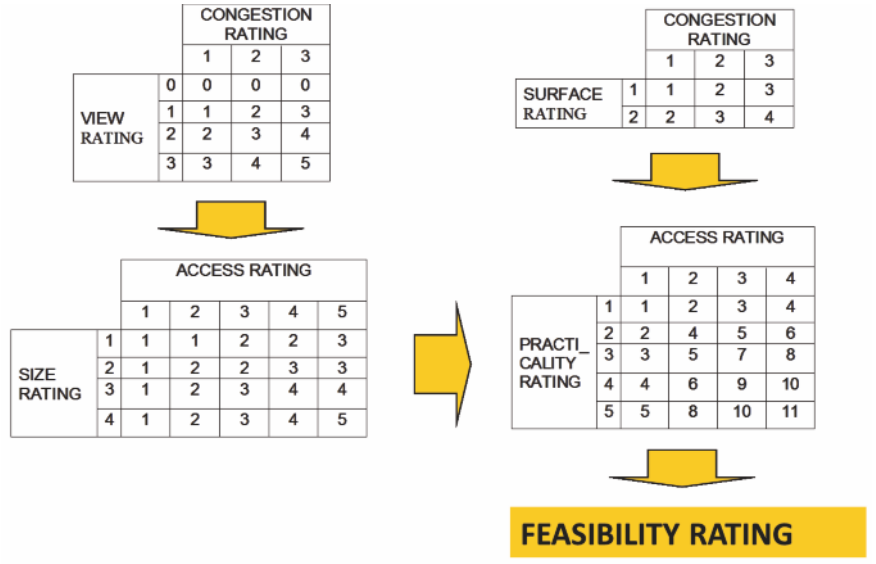

Figure 34. Rating scheme to determine feasibility ratings in damage tolerant structural design

To determine the initial crack length detectable in a damage tolerant structure a fairly systematic rating procedure has been introduced which is shown in Figure 34. The procedure starts from assessing a congestion rating (the degree of congestion where the component is placed) on a scale between 1 and 3 and a viewing rating (the degree a damage critical location can be viewed) on a scale between 0 and 3 and correlating the two ratings to a new rating called the access rating. This access rating is then further correlated to a size rating (size of the component considered) which then results in a practicality rating. Furthermore the congestion rating considered before is additionally correlated with a surface rating (surface condition of the damage location considered) which results in another access rating. This latter access rating is finally correlated with the practicality rating determined before and results in a feasibility rating, a number which ranges between 1 and 11 and is an indication of the initial crack length to be assumed. An indication of those initial crack lengths versus the feasibility ratings is provided in Figure 35 and shows that those initial crack length can go up to a size of 300 mm easily. The initial crack length determined from Figure 35 is what is also called the basic crack length L_{BAS}.

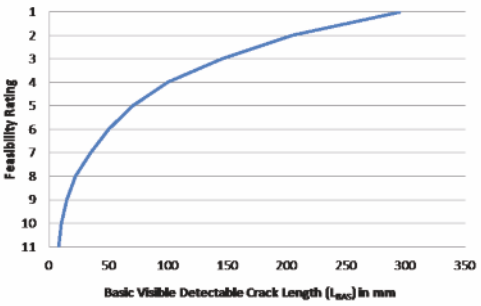

Feasibility Rating	L_{BAS} [mm]
11	8
10	10
9	15
8	22
7	35
6	50
5	70
4	100
3	145
2	205
1	295

Figure 35. Correlation between feasibility ratings and initial crack lengths for damage tolerant design

L_{BAS} may however not be the final crack length to be considered, as can be seen from the example shown in Figure 36. L_{BAS} may therefore be further multiplied by a gauge effect and an edge effect which are based on the following:

Gauge effect

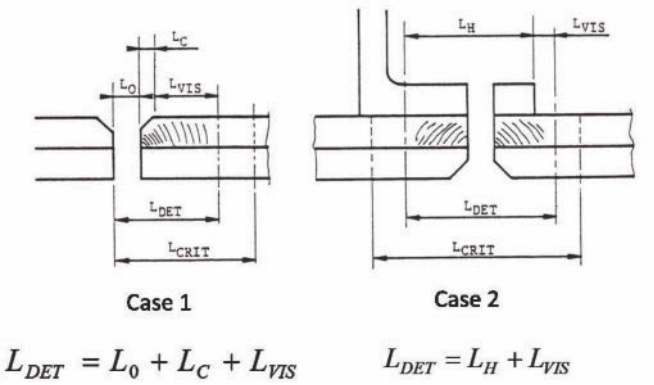

Figure 36. Definitions of a detectable crack length L_{DET}

The thicker the material of an item the tighter a crack is held together and therefore the more difficult it is to detect. To cater for this the basic detectable length is adjusted as follows:

1. for material thickness < 5 mm: multiply by 1
2. for material thickness 5 to 10 mm: multiply by 1.25
3. for material thickness > 10 mm: multiply by 1.5

Edge effect

For cracks which originate from or terminate at the edge of a member the detectable length is to be multiplied by 0.5, for non-edge cracks by 1.

Considering the following definitions

L_{BAS}	Basic visible length
L_{VIS}	Visible detectable length = $L_{BAS} \times$ gauge effect $\times$ edge effect
L_{CRIT}	Critical crack length
L_C	Concealed crack length (e.g. under fastener head or other fitting)
L_0	Effective crack length due to hole (as determined by stress office)
L_H	Hidden crack length

a detectable crack length L_{DET} can be calculated which is the initial crack length for a crack propagation calculation to follow which allows crack propagation life and hence an inspection interval to be determined. It is amazing to note that such an initial crack length could be up to 500 mm in the most critical circumstances. This demonstrates what potential damage tolerant design might have in designing engineering structures lighter weight.

3.3 SHM, Loads Monitoring and Damage Tolerance

The application of the damage tolerance design principle requires the load sequence applied to be known. Knowledge of the load sequence can be achieved by assuming the load sequence in accordance the different standard load sequences having been generated over the past and where new standard load sequences are still generated for different new applications. Those load sequences have to include a respective safety factor such that they do not generate any critical assumptions. The standardized load sequences provided do usually refer to a single location on the structure only such as a location around the centre of gravity in the case of an aircraft or the attachment of the wing. However would those load sequences also apply

to any other location on the aircraft, say to a fitting at the nose landing gear? In that case it might be more advisable to place a sensor at the specific location considered. With SHM this is possible today. A fibre Bragg grating sensor might be easily placed at the location of interest and the real operational load spectrum could be used to evaluate damage accumulated and the location where damage might be due to occur. This way of local loads monitoring would also help to better determine the incident when damage would have to occur as well as potential inspection intervals in terms of damage tolerant design when compared to a global loads monitoring such as around the centre of gravity. However it has to be kept in mind that damage initiation and accumulation is a process driven by a significant amount of statistical parameters. It is therefore useful that loads monitoring based fatigue evaluation procedures can be used to determine the locations prone to fracture around which then a sensor system can be placed that effectively monitors critical damage occurring in accordance to the damage tolerance criteria set. This approach does also guarantee an optimum usage of sensors to be integrated onto the structure to be monitored and provides an optimum strategy with regard to the SHM concept applied.

4 Non-Destructive Evaluation – Some Basic Principles

4.1 Historic Background

Non-destructive testing (NDT) is a science which correlates physical properties to materials' and structural conditions. Historically this correlation is known for thousands of years. Around 8,500 years ago acoustics was determined as a phenomenon for monitoring, followed by magnetism and temperature around 3000 years ago. It is however only during the last 200 years where those phenomena have been converted into what we are considering as science today. In the early 19^{th} century vibration analysis was introduced by individuals such as Fourier, followed by magnetism through Faraday in 1831, radiography by Röntgen in 1895 or dye penetrant around the same time. It is amazing that ultrasonics as a science only dates back to the 1920ies, followed by nuclear magnetic resonance in 1938 and recognised by awarding the Nobel prize to Rabi (in 1944) and Bloch and Purcell (in 1952). It is only in the 1980ies where giant magnetic resistors were discovered with the Nobel prize awarded to Grünberg and Fert in 2007. NDT is therefore a fairly young area of research.

SHM has inherited a variety of the NDT techniques developed with regard to damage monitoring so far. NDT techniques may be categorized

into standard and non-standard techniques as to Table 3 below. From those some of them are known to be used within the context of SHM where others are still mainly undiscovered within the SHM context. Table 3 therefore summarises NDT techniques with SHM potentials.

Within SHM partially a different or more specific wording is used for literally the same thing. The NDT techniques with SHM potential determined in Table 3 are therefore compared to some popular SHM terms along Table 4. What turns out is that a variety of specific techniques have been selected less systematically in SHM than this is now established in NDT. Some of the NDT principles can therefore be found in SHM, however there is still much potential for SHM to be explored in NDT where a few examples are explained in more detail in the sub-chapters to follow.

4.2 Magnetism

Magnetism is a physical parameter inherent to any ferro- and even paramagnetic material. It can be measured by inducing a magnetic field into the component to be monitored and sensed by the resulting magnetic response in accordance to the principle shown in Figure 37. This will allow material properties to be monitored up to a specific depth depending on the magnetic field to be introduced as well as effects (i.e. cracks) to be observed on the specimen's surface.

Microstructure of a magnetic material is composed of domains which can be considered as small magnets arbitrarily oriented in the specimen considered in case the specimen has not been considered as a permanent magnet. Those domains are separated by Bloch walls which are nothing

• **Standard**	• **Non-Standard**
– ***Visual***	– ***Acoustic Emission***
– ***Vibrations***	– ***Magnetics***
– ***Ultrasonics***	– Nuclear Magnetic Resonance
– ***Eddy Current***	– ***Microwave/Radar***
– X-Ray	– ***Optical Coatings***
– ***Thermography***	– ***Nanoagents/-coatings***
– Microscopy	

Table 3. NDT techniques with SHM potential (in bold italic)

• **Acoustics**	• **NDT with SHM potential**
– Guided Waves	– ***Visual***
– Acoustic Emission	– ***Ultrasonics***
– Piezoelectric Transducers	– ***Acoustic Emission***
• **Eddy Current**	– ***Vibrations***
– EM Foils	– ***Magnetics/Eddy Current***
• **Modal/Vibration Analysis**	– ***Thermography***
• **Miscellaneous**	– ***Optical Coatings***
– Thermal	– ***Nanoagents/-coatings***
– Comparative Vacuum Monitoring	

Table 4. NDT techniques associated with SHM

else than a sharp conversion of the electrons' orientation with regard to each of the neighbouring domains' magnetic orientation. Bloch walls are 'pinned' to lattice imperfections within the material would those imperfections be dislocations, precipitates, grain and phase boundaries or any other type of imperfection. If a magnetic material is exposed to a magnetic field the way this is shown in Figure 37 Bloch walls will gradually move and jump from one imperfection to the next leading the domains to gradually orient towards the magnetic field being imposed. This process of enforced reorientation continues with increasing magnetic field until a saturation level is achieved along which all domains are finally oriented in the direction of the enforced magnetisation. Figure 38 shows schematically how the magnetisation process is introduced and three stages of such a magnetisation process in form of some microscopic images can be seen in Figure 39. Once the magnetic field imposed is again reduced Bloch walls and domains do gradually establish again and the process might be inverted in case the magnetic field will be oriented into the opposite direction. This does result in a hysteresis loop like the one shown in Figure 40 which correlates the magnetic field H generated versus the magnetic flux density B generated in the specimen. Further details on magnetisation of materials can be found in textbooks such as [21,22].

Studying phenomena of magnetisation along the hysteresis loop shown in Figure 40 in more detail will elucidate a variety of interesting phenomena. First of all the shape of the hysteresis loop itself is a characteristic where the value at zero magnetic flux is considered as coercivity and the value of

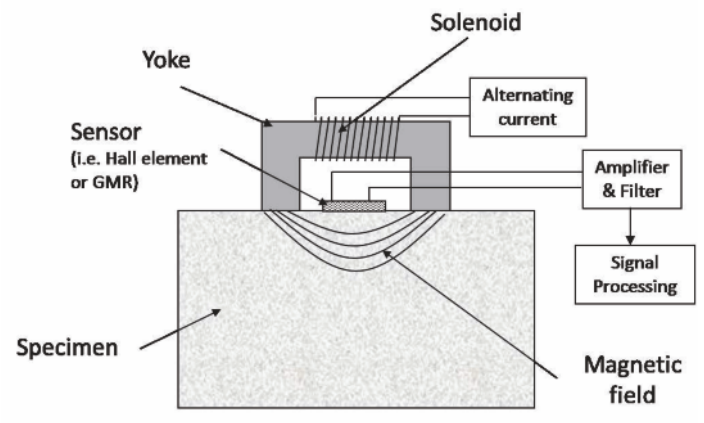

Figure 37. Working principle of magnetics monitoring

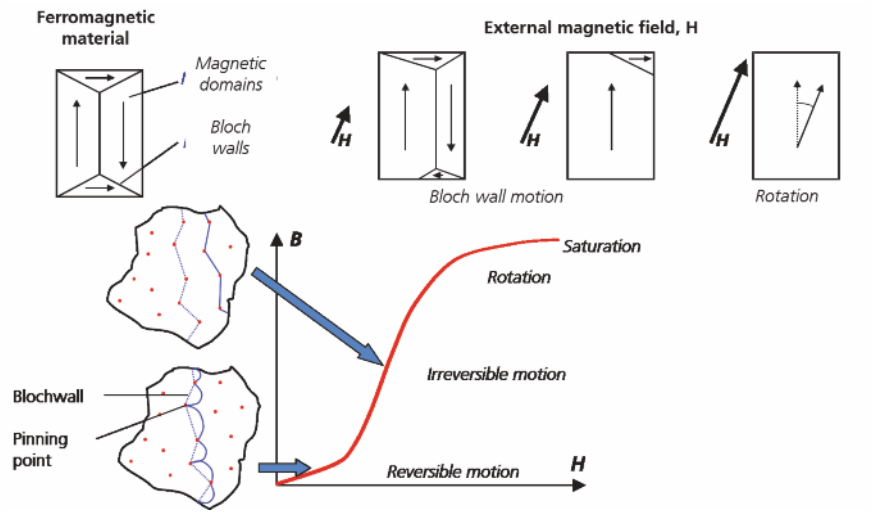

Figure 38. Bloch wall distribution and initial magnetic hysteresis curve in accordance to the four domain model by Cullity (21)

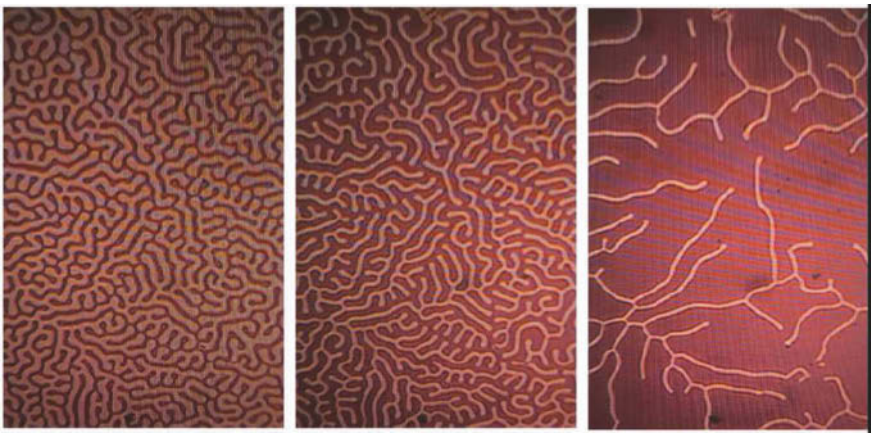

Figure 39. Change of domain structures with increasing magnetisation (from left to right)

zero magnetic field as remanence respectively. It can be further observed that Bloch wall movement at the higher magnetisation scales as well as at rotation processes of electrons around the saturation level are both stress sensitive.

Stress sensitivities may also be observed around the point of coercivity (BW2) in an indirect way. The phenomenon observed in that region is Barkhausen noise for which the principle is shown in Figure 41. Barkhausen noise is generated when Bloch walls move uncontinuously from one imperfection to another and this movement generates pulsed eddy currents to be measured by a sensor which need to be adequately amplified. The resulting output signal is currently characterised by its amplitude and also envelope. When performing a Barkhausen noise test on a specimen being exposed to different loads and hence stresses a change of the maximum amplitude of the Barkhausen noise signal is observed as can be seen from the results shown in Figure 42. Furthermore the field strength where this maximum occurs may change too, which also becomes obvious when looking at the shape of the magnetic hysteresis loop being generated since the maximum of the Barkhausen noise is correlated with coercivity in a large number of cases. Plotting the maximum of the Barkhausen noise signal over the stress applied on the specimen leads to a low scattered non-linear relationship (23). Reasons for this non-linearity are various where magnetostriction may be one with others being subject of on-going and future research.

Since electromagnetic and magneto-elastic quantities of a ferromagnetic

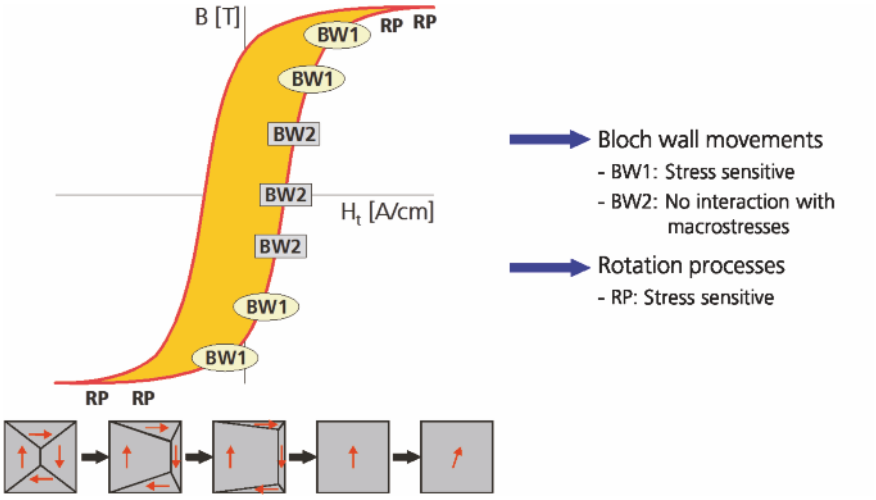

Figure 40. Typical magnetisation hysteresis loop

material are influenced by stress and microstructure and any resulting changes from this, a calibration may be considerable. This may be achieved on either a tensile or bending test. A one dimensional calibration based on magneto-elastic Barkhausen noise measurement is usually sufficient where the amplitude of the magnetic Barkhausen noise is measured as a function of the tension and compression applied to the specimen. This calibration seems to be sufficient as long as the stress in the second principal direction is less than about 25% of the elastic limit of the material. Otherwise biaxial calibrations have to be performed (24) or a calibration procedure based on specific calibration functions as described in (25).

Besides Barkhausen noise and the shape of the hysteresis loop and hence magnetic permeability being the derivative of the hysteresis loop in general there are two further magnetization effects of significance where one of them is the impedance measurement of an induction coil known as a parameter from conventional eddy current testing and the other is higher harmonics analysis. Higher harmonic analysis of the tangential field strength is the magnetic response signal resulting from an external magnetic field excitation alternating at a specific frequency and being measured as a response signal from the component analysed in terms of a fast Fourier transform analysis, resulting in a harmonic distortion factor mainly considering the first odd harmonics. All of those magnetics phenomena are summarised in the chart shown in Figure 43 below. Looking into further details Fraunhofer IZFP

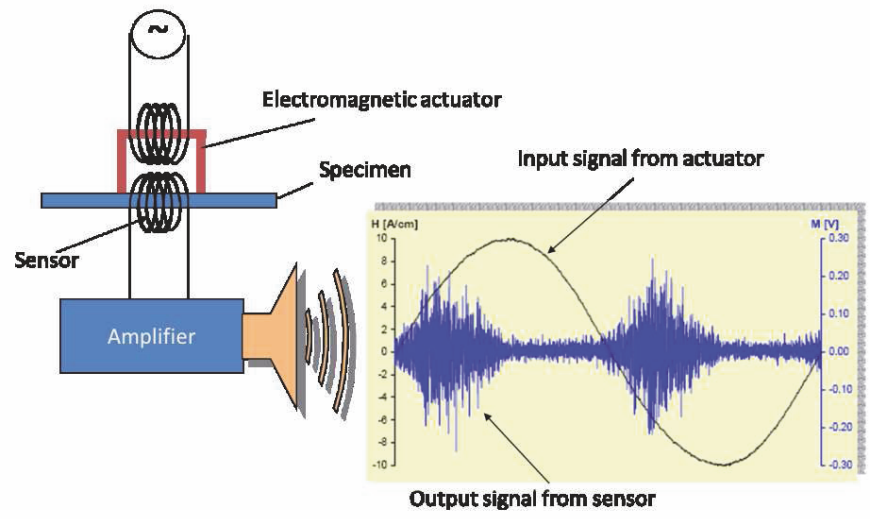

Figure 41. The Barkhausen noise principle

has identified up to 42 parameters in that regard which are selected and tuned in accordance to the specific application to be considered (26).

That micromagnetic techniques can be efficiently used for monitoring ageing structures which has been clearly shown in the case of a steam pipe material (27) that can burst due to ageing phenomena. The steel pipes made of WB36 and operated at temperatures around 350 °C generate copper precipitates over time and results in a significant increase in hardness, brittleness and hence fracture stress intensity. Those copper precipitates are excellent pinpoints for Bloch walls and may be indirectly measurable through the Barkhausen noise being generated as shown as a principle in Figure 44. That the assumption of correlating magnetic with mechanical hardness has indeed become true has been validated experimentally where material of the WB36 steel pipe has been continuously aged and hardness increase measured has been compared to the micromagnetic signals monitored. Results of this comparison are shown in Figure 45 and a good correlation can be observed which recognises micromagnetics already as a promising technique for monitoring ageing phenomena in magnetic materials.

As already explained in the context of Figure 40 micromagnetic techniques are also sensitive to stress measurement. This has made those techniques attractive for stress measurement in deep drawing steels such as

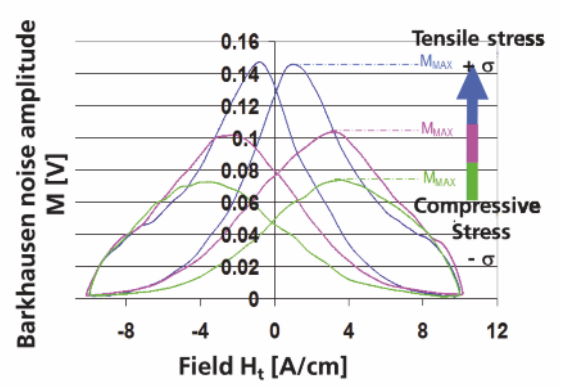

Figure 42. Barkhausen noise sensitivity to applied stress under uniaxial loading

used for automotive structures. Figure 46 shows a comparison of residual stress measurement on formed sheet metal for automotive application and demonstrates the significant advantage micromagnetics has when compared to radiography.

Sensing with micromagnetic techniques is traditionally done with a coil or possibly even a Hall sensor. A significantly emerging alternative is however the use of giant magnetic resistors (GMR), which have become a standard in all kinds of electronic data communication and specifically data storage devices such as harddisks. As schematically shown in Figure 47 a GMR is a composite system consisting of at least two ferroelectric layers switched in opposite directions and separated by an electrically conductive paramagnetic layer. For an antiparallel configuration of the electron spin orientation the electrical resistance is high and hence any impedance measured when placing the GMR sensor in an electromagnetic field will become high as well. Figure 47 shows on the right hand side the size of such a sensor (in that case of four sensors due to a Wheatstone bridge) which demonstrates that such a sensor could be implemented in damage critical notches of fairly small size.

Monitoring structural components with GMR sensors has provided some interesting results where some have been published in (28). One of those examples is shown in Figure 48 and demonstrates that electrical impedance measured by a GMR sensor system can be well correlated to plastic strain

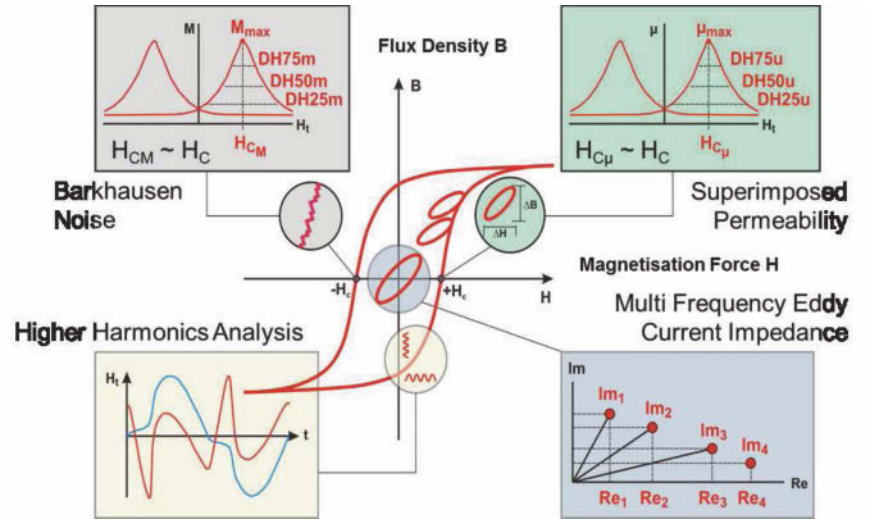

Figure 43. Magnetic hysteresis curve and magnetic phenomena considered

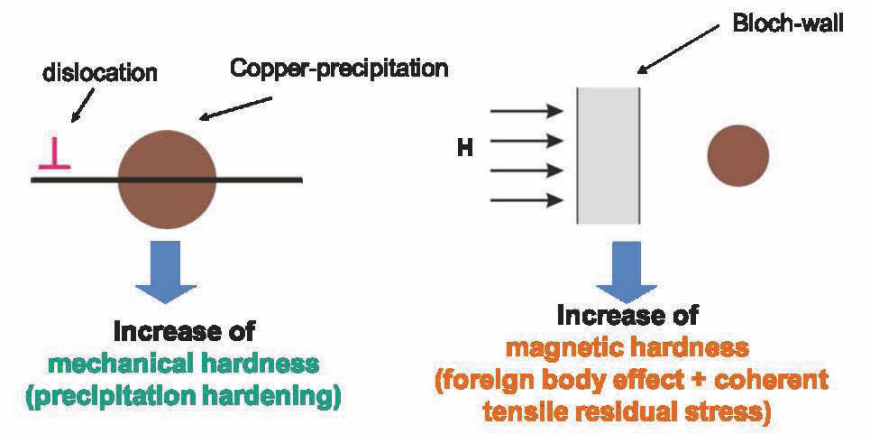

Figure 44. Analogy between dislocation movement due to mechanical loads and Bloch-wall movement under magnetization

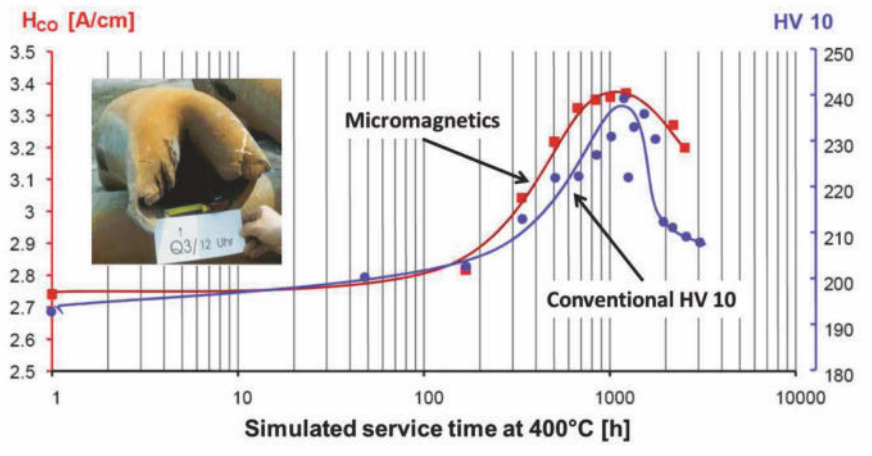

Figure 45. Analogy between mechanical and magnetic hardness

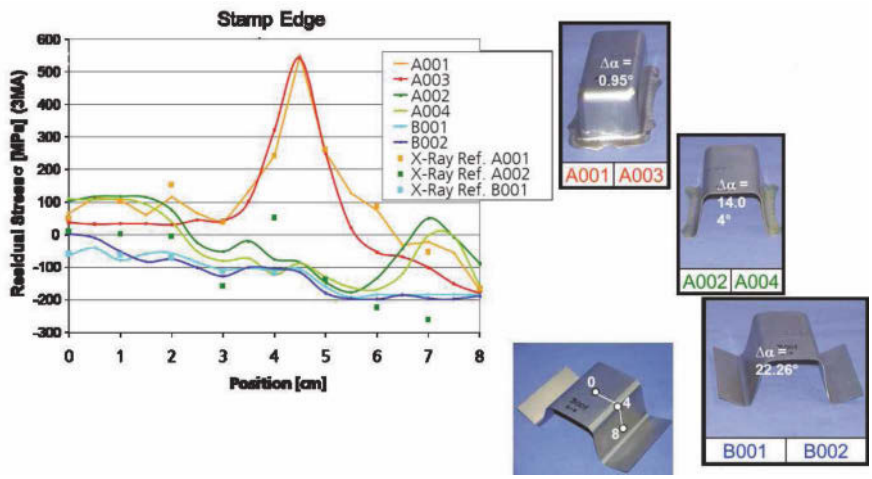

Figure 46. Measurement of residual stresses in formed steel using micromagnetics and compared to conventional X-ray analysis

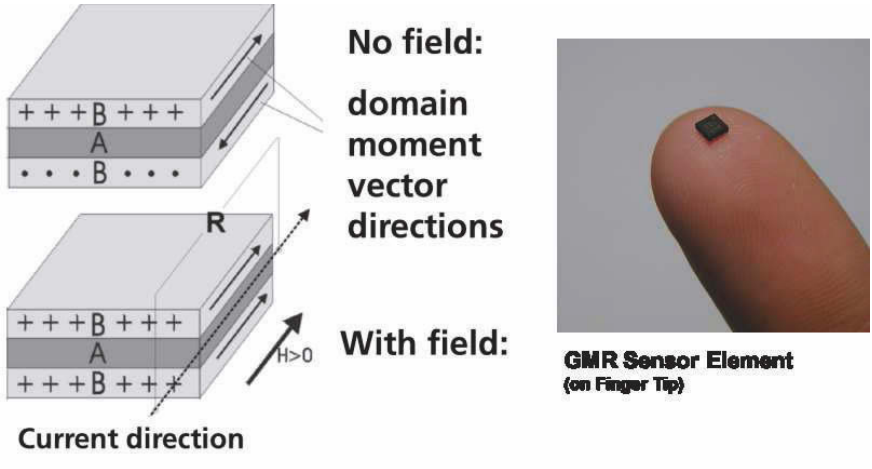

Figure 47. Giant magneto resistor (GMR) sensing device

being generated along a fatigue test under random loading.

All together micromagnetics shows a highly promising but far from being exhaustively explored area for monitoring ferro- and paramagnetic materials and structures. Since the technique is also sensitive to microstructural effects it can be used to determine material properties at the early stage of damage incubation too, much earlier than any crack monitoring technique does. An interesting correlation shown in Figure 49 below can therefore be principally observed on a microstructural level between micromagnetic values on the one side and mechanical values on the other.

4.3 Electromagnetic Ultrasound (EMUS)

The principle of electromagnetism shown in Figure 37 above can be also applied in a wider sense, such as generating an ultrasonic wave the way this is shown as an example in Figure 50. In this case the dynamic magnetostriction is generating an ultrasonic wave in addition to the magnetic properties described before, which can provide additional information of a component's condition, specifically when a larger volume of the component considered is intended to be monitored. This is what is also called electromagnetic ultrasound (EMUS). An interesting and also highly successful application is the examination of railway wheel rims as shown in Figure 51 below. In that case a Rayleigh (surface) acoustic wave is sent around the rim with echoes and through-transmitted signals being recorded. Any turn of the

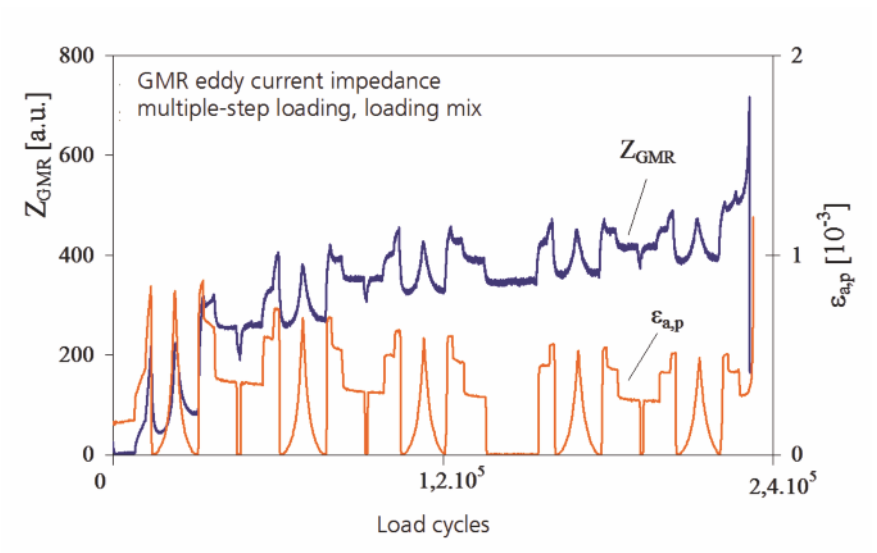

Figure 48. Plastic Strain Characterisation with GMR Sensors for AISI 321 Steel under Service Loading

signal around the wheel can be recognised through the time of the signal's flight while any imperfections on the rim are recorded by echoes observed in between. The EMUS actuation and sensing unit is placed within the rail and allows trains to roll over at speeds up to 15 km/h while the inspection process is performed. EMUS has also been successfully applied in the context of inspecting welded sheet metal such as tailored blanks, where guided waves are generated being sent through the sheet metal and being reflected by the weld in accordance to a defined condition. A major advantage of EMUS is its ability to generate shear horizontal waves which piezoelectric actuators are less able to do and the avoidance of a coupling medium which allows EMUS to be also applied at elevated temperatures.

4.4 Eddy Current

Eddy current is another electromagnetic technique applied. Instead of a yoke with a coil operating as a solenoid a simple coil is used to generate an alternating magnetic field through an alternating current. This will generate eddy currents in any electrically conductive material which can be measured by the electrical impedance. Figure 52 shows the principle

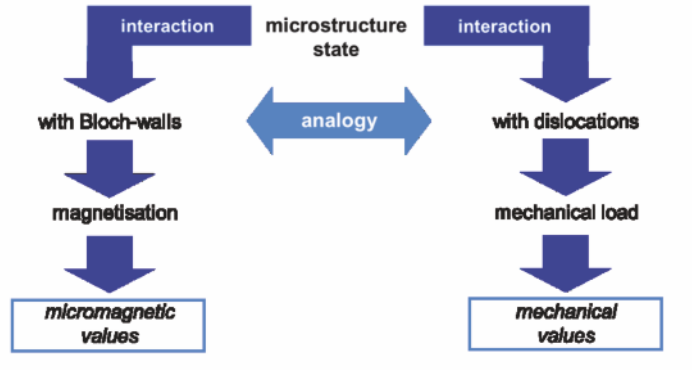

Figure 49. Correlation between micromagnetic and mechanical values

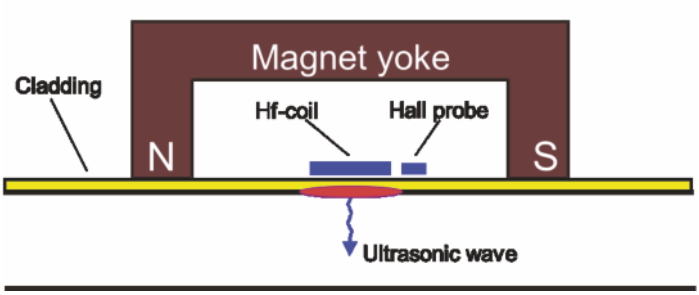

Figure 50. EMUS for monitoring a material's condition under a cladding

of eddy current inspection. Eddy current testing can be performed in a wide range of frequencies depending on the size of damage to be detected and the location of the damage below a surface. Principally the higher the frequency becomes the smaller a defect can be detected and the lower the damage below the surface can be. Eddy current testing may also be used for monitoring the thickness of coatings.

Eddy current testing has been traditionally used for the inspection of metallic materials. However this may also be used for other electrically conductive materials such as carbon fibre reinforced composites (CFRP). Recently a scanner has been developed shown in Figure 53 which allows for the inspection of CFRP materials up to a defined thickness using high

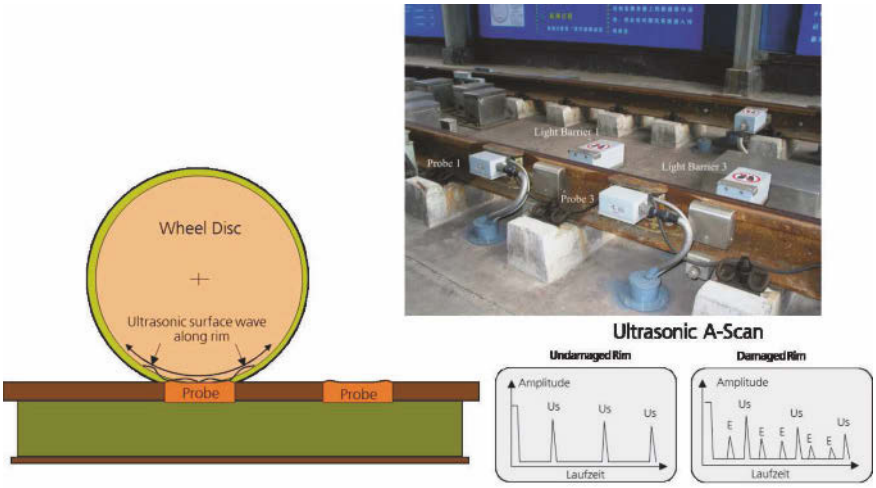

Figure 51. In-motion EMUS testing on railway wheel rims

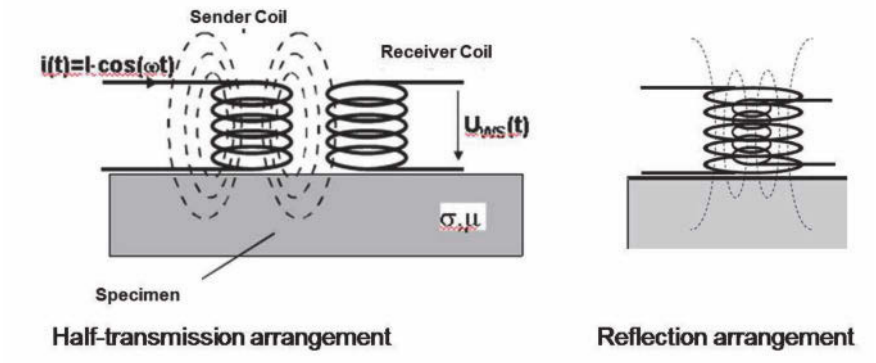

Figure 52. Principle of eddy current testing

frequency eddy current (29). The sensor being used is a very specific matrix sensor which allows for monitoring techniques to be used similar to what is known in the context of phased array techniques in acoustics.

Eddy current has been also applied in the context of SHM as eddy current foils where coil typed structures have been placed on Kapton foils which again could be placed on or between lap joints such as for corrosion detection (30).

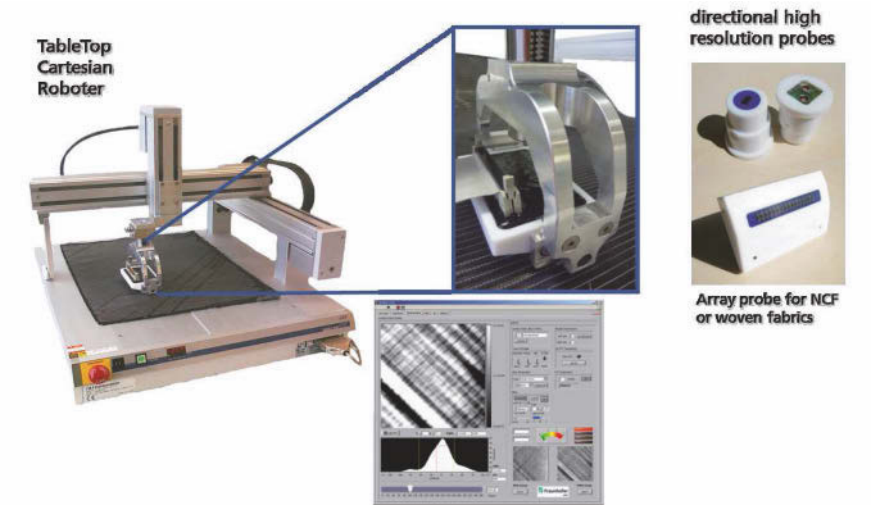

Figure 53. High frequency eddy current based scanner for CFRP testing (Courtesy of Fraunhofer IZFP)

4.5 Ultrasonics

Acoustics and hence ultrasonics using piezoelectric transducers is the physical principle possibly used most in NDT. Current emphasis is specifically on the use of phased arrays combined with advanced data management. A method in that regard principally shown in Figure 54 is sampling phased array where a signal is sequentially sent by one of the transducers and the echo is recorded by all the others. All time domain data generated is stored in a data base which is then taken as a basis to determine an optimum spatial and contrast resolution by calculating the image recorded mainly through phase shifting and the Synthetic Aperture Focusing Technique (SAFT). Images obtained in near to real time are 3D volumetric pictures of high resolution as shown as an example in Figure 55. This approach may also be used in the context of SHM where transducers are sparsely distributed around a structure and the resolution of images obtained may be enhanced.

4.6 Other Conventional NDT Techniques and Emerging Technologies

There is a variety of other NDT techniques widely considered in structural inspection. One of them is thermography where a heat impulse such

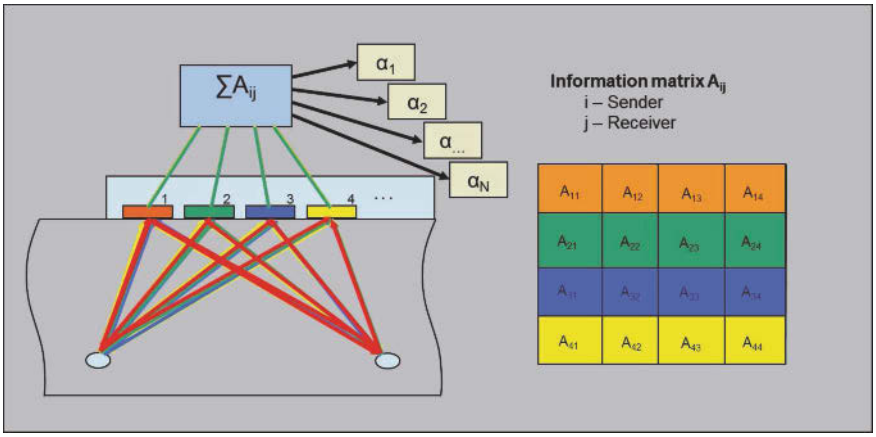

Figure 54. Data sampling procedure using the sampling phased array principle

as generated through a halogen lamp is sent into the structure to be monitored and the temporal change of the reflected temperature signal is integrally recorded by a camera system such as an IR camera (Figure 56). Any changes in the material's condition due to defects may be observed through a change in density, heat conductivity and specific heat capacity observed by a change in amplitude, phase or even both being measured. Heat actuation may be also generated through vibration such as a sonotrode or some multi-use sparse piezoelectric transducers within the structure being considered. Another alternative explored is local heating by a laser. The advantage of thermography is its integral, non-contact and non-invasive way of monitoring which makes it attractive for any high speed monitoring. However resolution may still have to be enhanced where current research still demonstrates significant margin for improvement.

Another NDT-technique being highly popular for quality assurance purposes is radiography as shown as a principle in Figure 57. The object to be inspected is exposed to x-ray radiation while the projection image is recorded by a digital image recorder. Since the object is turned around on a manipulator data acquisition is performed for a variety of different angles. Through data processing and use of a computing tomography algorithm a 3D image is generated which allows the size and volume of a damage to be determined quantitatively. X-ray sources are currently more and more placed on robotic systems which provide further inspection flexibility when the image recorder can be moved around accordingly such as shown with

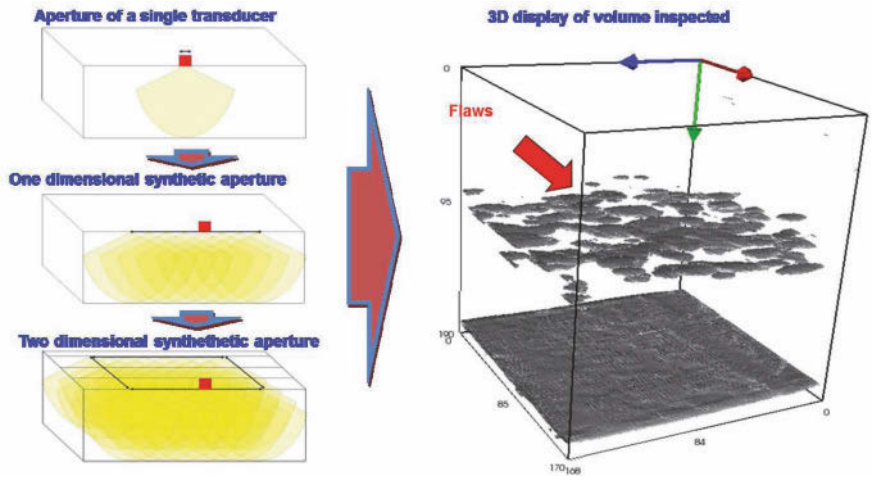

Figure 55. Quantitative 3D imaging using the sampling phased array approach

laminography in Figure 58. However due to being invasive radiology can be used as a validation method for SHM only.

Beyond all this there is a multitude of other optical techniques to be explored would those be based on planaroptical microresonators, optical coatings or any type of nanoparticles influencing fluorescence, all of those components to be adapted or integrated into the structural material considered. Doping structural materials with damage sensitive elements is a current trend in materials research ongoing with significant expectations regarding the future.

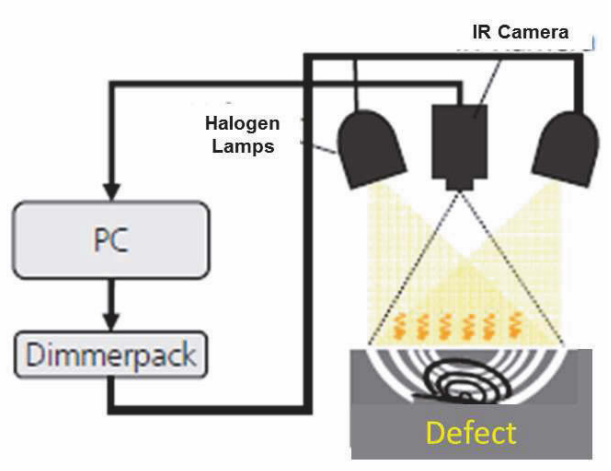

Figure 56. Principle of lock-in thermography testing

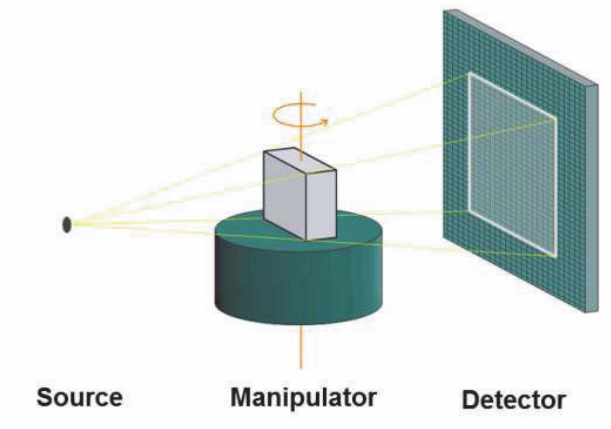

Figure 57. Principle of x-ray testing

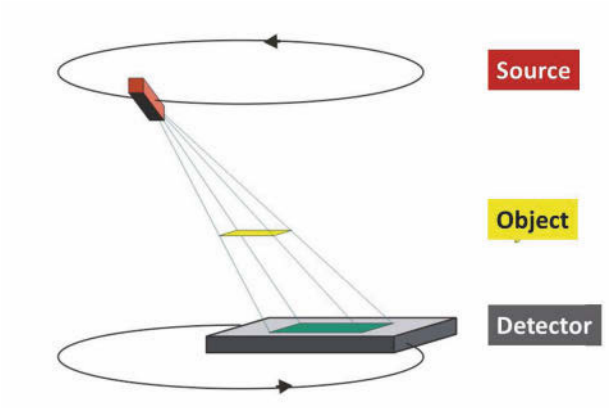

Figure 58. Laminography as a new way of x-ray inspection

5 Non-Destructive Evaluation in Composite Materials

The increasing request for glass and specifically carbon fibre reinforced plastic (CFRP) materials not just in aviation but recently also in the automotive sector has triggered a lot of thought for further improvement of NDT techniques to be used. Current testing equipment is rather bulky, costly and specifically time consuming. Techniques used so far in aviation are ultrasonic testing (UT) and radiography based. Furthermore damage mechanisms in composite materials are much less known when compared to metals. Hence a safety factor has to be imposed along the design of those CFRP-structures as long as damage mechanisms are not sufficiently known and a damage tolerance principle cannot be applied. The objective of NDT for CFRP structures is in enhancement of flaw detectability and quantification, reducing inspection time and cost.

When looking at state-of-the-art NDT testing for CFRP structures, ultrasonic based phased array testing is the procedure most commonly used. X-ray testing, mainly on a computer tomography (CT) basis, is fairly exact but a costly and time consuming NDT procedure which is therefore considered for verification purposes only. There are other NDT techniques considered as well, however they have not been approved in many fields of application (i.e. aviation) due to lack of certification so far. To better understand the current state-of-the-art in CFRP-related NDT technology a benchmark test has been performed. Driven by leading edge technology

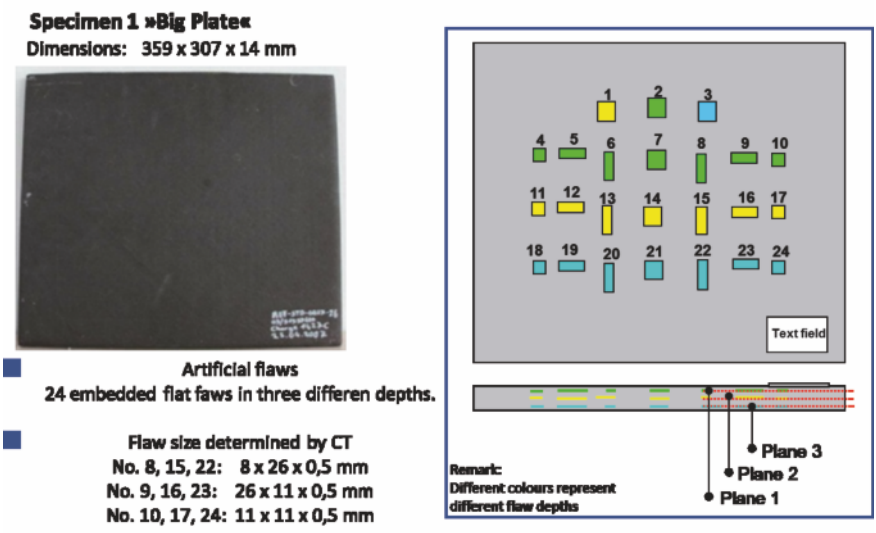

Figure 59. Plate with flaws of different size and at three different depths (Specimen 1)

such as sampling phased array in the case of UT and 3D imaging algorithms in the case of radiography, those two traditional techniques have been compared to emerging NDT techniques in the CFRP field including thermography and eddy current testing. The components considered for validation have been mainly stepped flat panels with integrated artificial flaws such as shown in Figures 5.1 to 5.4 respectively.

Results obtained in detecting the various flaws are summarised in Table 5. None of the specimens were a challenge for the two 'classical' NDT techniques being phased array UT and x-ray CT where 100% of the flaws were detected with even excellent resolution. Specifically UT benefitted in resolution from using sampling phased array. Flaws in the knee point of specimen 4 could be detected after a sensor head was used that was in accordance to the specimen's geometry, being an indication of UT limitations with regard to increased complexity of a component's geometry. Limitations with x-ray CT has to be seen in the weak distinction between material densities and also the high effort required in general would it be time, cost and safety. However space is also a limitation if a conventional CT-equipment is considered to be used.

The major reason why high frequency eddy current (HFEC) and ther-

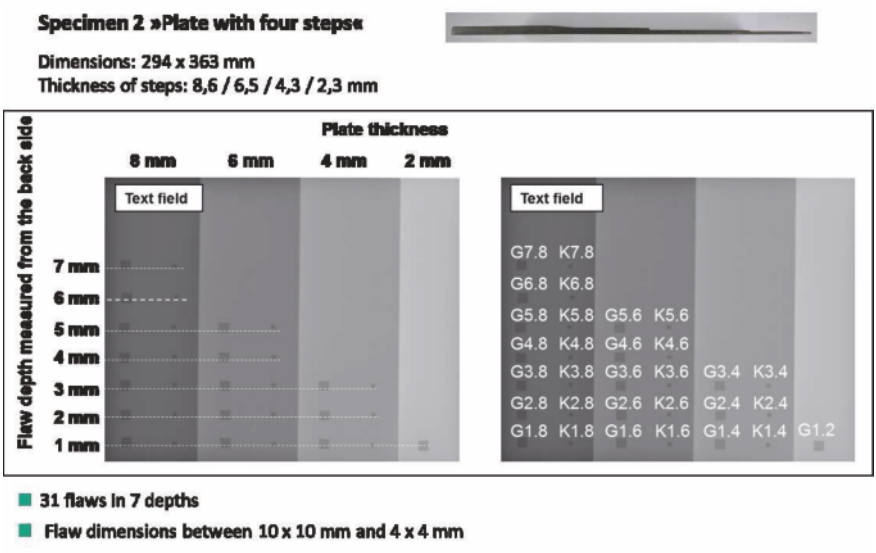

Figure 60. Four stepped plate with same sized flaws at different depth (Specimen 2)

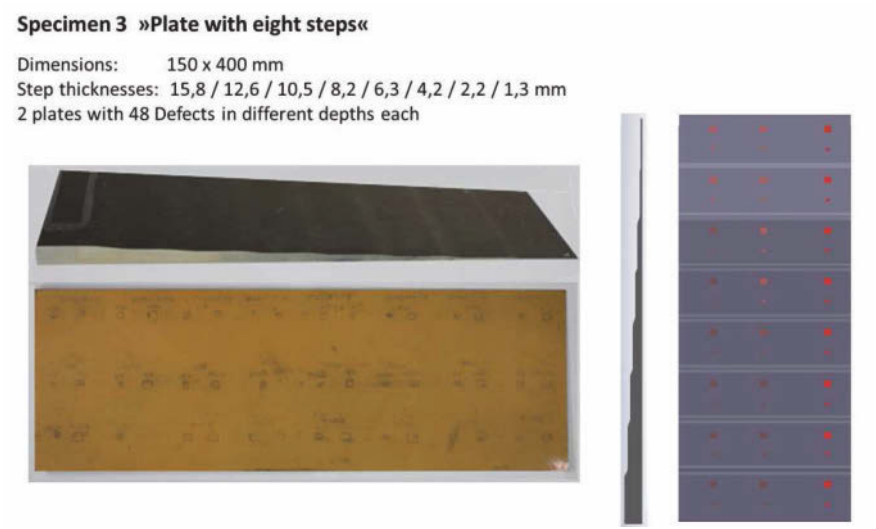

Figure 61. Eight stepped plate with same sized flaws at different depths (Specimen 3)

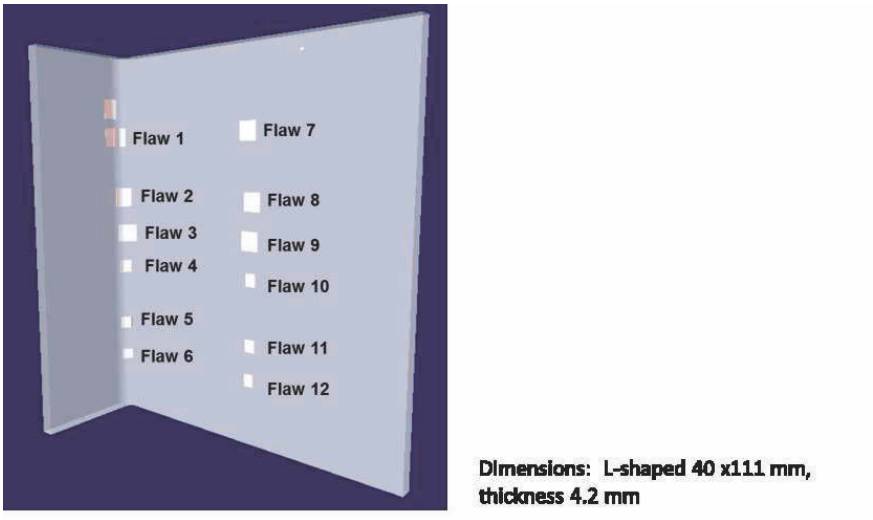

Figure 62. L-shaped clip type specimen with different flaws at three different depths (Specimen 4)

mography have only been able to detect a little more than half of the flaws results from the fact that their resolution in depth is very much limited. So far this is limited to about 7 mm in depth. Results can be improved if the specimen is allowed to be inspected from two sides. Further limitations mentioned in Table 5 currently still prevail. HFEC and thermography have other significant advantages when compared to UT and CT where non-contact sensing in case of both and large space monitoring in the specific case of thermography have to be mentioned. A summary of various advantages and disadvantages of the different NDT-techniques considered is provided in Table 6.

Since inspection time is a critical parameter in CFRP component manufacturing a slightly more detailed look has been placed on this parameter. A 30 x 30 cm CFRP panel has therefore been selected as a reference being slightly similar to the larger specimens 1 and 2 discussed above. Although that comparison could not be made in all details a time target was at least set such that inspection time would be achieved below 30 seconds. Results from that comparison can be seen in Table 7. Current state-of-the-art technology shows that inspecting a component of the respective size is a matter of minutes. UT can so far only benefit from phased array testing and high performance signal processing and hence computing and has significant po-

NDT method	Flaws detected %	(Physical) limitations
UT / SPA	100 % (163/163)	- Complex geometry
CT	100 % (163/163)	- Weak distinctions in density
EC	52.8 % (86/163)	- Weak distinctions in conductivity especially in depth direction - Only flaws near the surface
Thermography	54.8 % (86/157)	- Weak distinctions in density, heat capacity and heat conductivity - Only near surface flaws detectable; - Rule of thumb: lateral dimensions > depth

Table 5. Results of NDT-technique benchmark on CFRP specimens

NDT method	Advantages	Disadvantages
UT / SPA	3D volume capture High flaw detectability Quantitative flaw evaluation	Coupling is required – complex mechanics Significant equipment costs for complex geometries
CT	3D volume capture High flaw detectability High spacial resolution Quantitative flaw evaluation	Limitations on object size Significant equipment costs
EC	Fast, flexible, coupling free Low cost equipment High potential for automation	Limited sensitivity Limited depth range Only qualitative detection, flaw depth/size can only be estimated
Thermography	Simple testing procedure (no contact, less scanning) Fastest possible testing for large components and also complex geometries	Limited sensitivity Limited depth range Only qualitative detection, flaw depth/size can only be estimated

Table 6. Advantages and disadvantages of NDT-techniques benchmarked

NDT method	Pure inspection time without arrangement	
CT CT Laminography	from 5 min to 30 min < 30 s	(surface 30 cm x 30 cm)
UT / SPA	< 30 s	(surface 30 cm x 30 cm)
Lock-In thermography	ca. 100 s – 400 s	(surface 30 cm x 30 cm)
Pulsed thermography	< 30 s	(surface 30 cm x 30 cm)
EC	< 30 s	(surface 30 cm x 30 cm)

Table 7. Benchmark related to inspection time of a laboratory based component

tential to meet the time target set. With CT laminography will be the method of choice helping to speed up the process while for thermography pulsed thermography may become the preferred method to choose. HFEC will easily meet the target specifically when matrix sensors will be used and the variety of signal processing options will still have been explored to their full extent.

In general it can be concluded that there is still a huge potential in enhancing NDT-based CFRP inspection which will allow inspection effort to be reduced by factors and times possibly too. These enhancements will certainly have a significant impact on further techniques to be applied with SHM and it is advisable to observe developments made in NDT and vice versa.

6 Approaches to Structural Health Monitoring

Although there is a lot of options available to get SHM established there are still a variety of open questions to be answered to get SHM implemented in the first place. Frequently asked questions in that regard may include: What does SHM cost? How to establish SHM? When to establish SHM? When will SHM pay off? This chapter tries to give some answers.

SHM is not something completely new. In aviation SHM was recognised after the serious Comet accidents in the early 1950ies although nobody used the expression of SHM at that time. Acceleration sensors were implemented on fighter airplanes and load spectra were continuously tracked, which then resulted in a variety of standard load sequences to be used for aircraft qual-

ification [7,31]. Today a modern fighter aircraft like Eurofighter Typhoon has a 16 strain gauge operational loads monitoring system which allows real load sequences to be tracked and damage accumulation to be determined. Similar approaches are made with bridges and other load critical structures and components. With the development of optical fibre Bragg sensing a completely new option of sensing has been provided that allows complexity of sensing to be reduced by orders of magnitude. One hundred conventional strain gauges with two wires each can now be easily replaced by a single fibre, giving rise to a multitude of interesting new applications.

A major rule in implementing SHM must be: *Maximise a SHM system's efficiency by minimising the number of sensors to the most efficient ones.* Sensors are only a part of an SHM system, which contains much more. A major element of an SHM system is simulation, which can be large computational machines not doing anything else than simulating the performance of a structure under various conditions. This simulation does require an input from sensors and the question is: *Which input will have which impact on an SHM system's performance output?* This is nothing else than an optimisation task which as a consequence asks for minimising the sensor's input to maximise a structure's performance output. In the case of SHM this means to start where structural design starts as well and this is with strength analysis of materials and structures. A strength analysis requires as an input material properties, the structure's geometric shape and operational loads. Material properties can be considered to be given, specifically when materials have been qualified through a quality assurance process. Geometric shape can also be considered to be given, where no change is to be expected over the structure's life. The only major unknown at this stage is operational loads, where assumptions are made prior to a structure's realisation and where safety factors have to be implemented to cover any unexpected uncertainties. Reducing those uncertainties is where sensors have to be implemented first and where major benefits can be expected due to the high safety (or better penalty factors) imposed initially. Determination of the type and sensors' best locations therefore has to come from the structural simulation process itself.

Once an optimum of loads monitoring sensors has been determined, placed on the structure and operating reliably safety factors can be reduced resulting in either lighter weight design and/or longer endurance, depending on what the operational target of the structure considered would be. A next factor of uncertainty within the structure's operational life is damage possibly combined with a change in the structural material's condition and the probabilistic nature of damage to occur. Again simulation might be a tool of major benefit although this time the tools might be more towards sim-

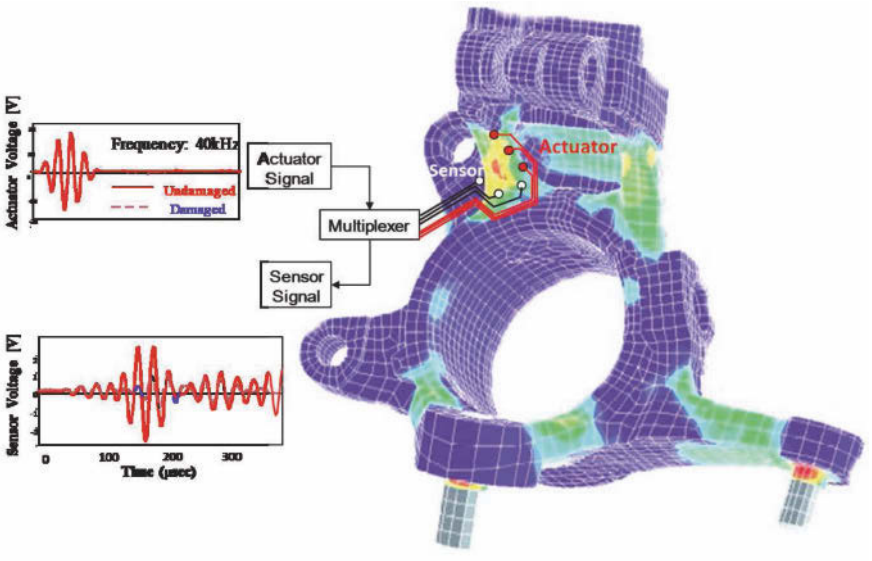

Figure 63. Fatigue life and damage evaluation to determine 'hot spots' for damage monitoring

ulation of materials properties on a molecular and possibly even atomistic level which might generate ideas for sensing other than those traditionally looked at in terms of strain monitoring. With all that information available from the load and material condition monitoring sensors as well as from the simulation algorithms applied locations of likely damage occurrence can be determined even on a prognostic level which will again allow an SHM-based damage monitoring system to be determined on a targeted and hence optimised level. An example for such a concept is shown in Figure 63 where a map indicating the locations ('hot spots') of highest damage accumulation is obtained through prognosis and hence simulation. It is for those 'hot spots' where simulation has then to be performed again, this time on the basis of simulating physical waves travelling around the hot spot and the allowable damage to occur such that the damage tolerated can be reliably detected with the NDT-based transducer configuration to be determined through simulation and successively then realised in hardware.

Although Figure 63 might imply that actuators and sensors or hence transducers might be the key elements of SHM this is by far not the case. What is essential with SHM is the SHM system. An SHM system as shown

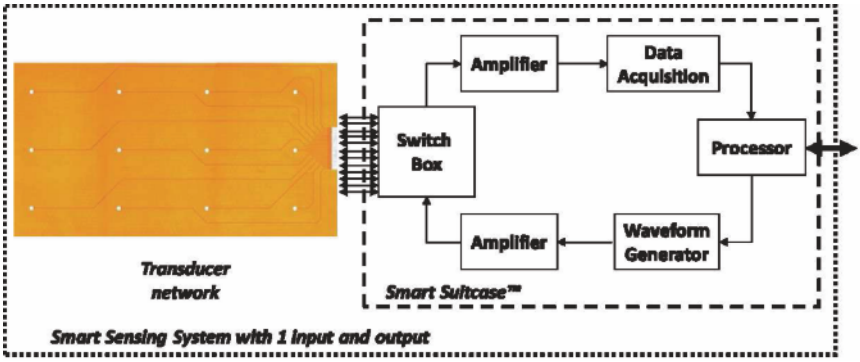

Figure 64. Principle of an SHM sensing system for damage monitoring

schematically in Figure 64 consists of a defined number of transducers which are managed by a signal generator, amplifiers, a multiplexer, a data acquisition unit and a processor. The most important requirement with this SHM system is that the single input and single output interface of the SHM system provides a reliability of information defined by the SHM system user requirements. If the rate of false alarms is set to 10^{-7} by the SHM system's user, then it is the obligation of the SHM system provider to get a system realised that will meet that requirement irrespective of how many transducers the system will need as long as the SHM system meets any other requirements set such as weight and cost.

Damage monitoring in aviation has been very much triggered by the Aloha Airlines accident which happened in April 1988. This accident made the public very much aware of a phenomenon called multi-site damage (MSD) which is when a structure suddenly fails like a perforated paper, because small cracks not fully detectable by means of NDT have been mainly generated at each of the rivets along a rivet line. As a consequence all aircraft types with an age of 15 years and more were analysed in terms of their damage critical components where additional care is required for those components with regard to damage tolerance which has resulted in enhanced inspection effort. This additional inspection effort is an interesting opportunity for SHM to be applied and it was therefore explored how well SHM might identify MSD along rivet lines. A substantial overview regarding all of this has been provided in (32) with a major conclusion, that cracks of 5 mm in length and above could be well determined with SHM when compared to conventional NDT. This was confirmed in a follow-on study (33) where the reasons for limited monitoring sensitivity with SHM were ana-

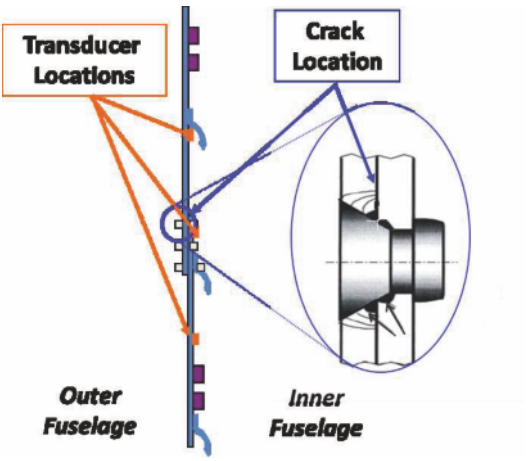

Figure 65. Acoustics based SHM on a riveted lap-joint panel

lytically explored and could be explained. A first explanation can be given when looking at the cross-section of a lapped joint of an aircraft and how an acoustic signal would have to travel as shown schematically in Figure 65. For pragmatic and possibly also aerodynamic reasons a monitoring unit might only be placed on the inside of the aircraft structure considered. The transducer layers were placed at decently separate locations mainly for the reason of being able to generate a fairly homogeneous guided wave. However this wave had to cross the lap and hence an interface which is a major source for attenuating the guided wave signal. Furthermore the area around the rivet is far from being of a simple shape. When a crack is therefore due to generate as indicated in Figure 65 it will start in an area where the interaction with the guided wave is by no means easily described nor even very much influential on the guided wave as long as the crack hasn't at least achieved a decent size.

Even when not considering the geometric complexity of a rivet hole the scattered signal resulting from a pure longitudinal Lamb wave generated is by far not as strong as one would believe. In (33) some simulation results shown in Figure 66 have been reported where a longitudinal wave has been sent through a plate with several holes and one of the holes had a crack of increasing length.

The top row of Figure 66 shows on the right hand side the intensity of the scattered wave distribution behind the hole for a quarter section

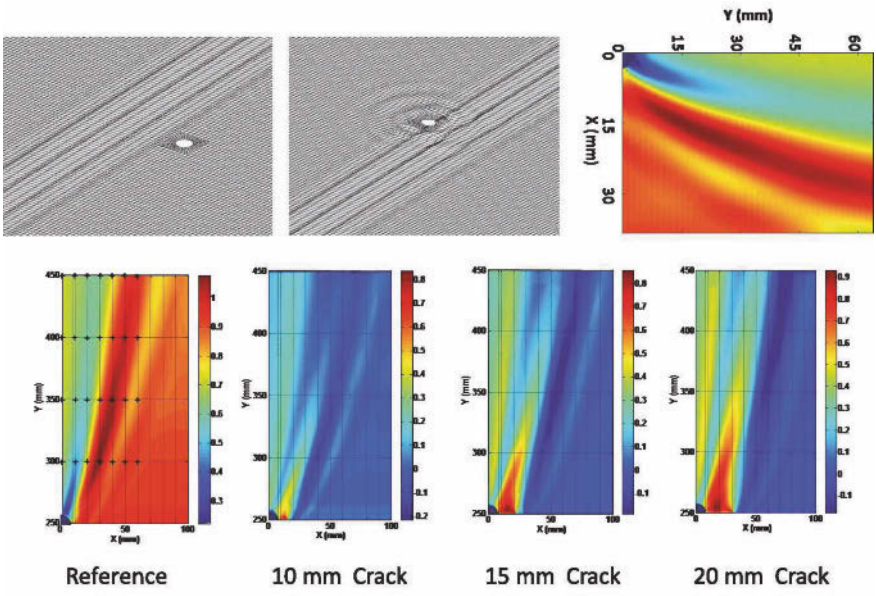

Figure 66. Influence of a hole in an infinite pate on the scattered wave behind the hole (top) and influence of a crack starting from the hole on the differential signal of the scattered wave (bottom)

only. It can be seen that the maximum distribution follows a hyperbolic distribution that fades away around 15 to 20 cm behind the hole. This signal shown also on the bottom left of Figure 66 has been taken as a reference for determining the difference to the signal determined for a crack emanating from this hole, shown on the bottom row of diagrams in Figure 66. It can be observed that the crack must have a substantial size to be detectable at a fairly still low distance to the hole and the crack itself. A rule of thumb can be set up saying: A crack length of 2.5 times the diameter of a hole (rivet) has to be monitored no further away than 12.5 times the size of the hole (rivet) diameter. This shows that damage monitoring is a 'hot spot affair' in all regards and that state-of-the-art SHM is currently possibly not able to detect damage of a size smaller than traditional NDT can do today.

However operators of damage tolerant structures might not show a very keen interest in getting damages detected at a size smaller than what has been considered to be tolerable. Within the world of structural integrity

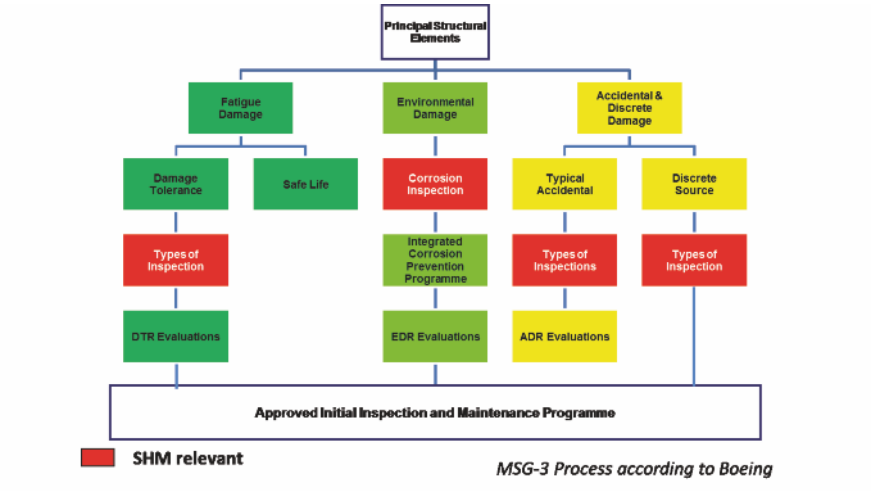

Figure 67. Options for SHM to go into the aircraft maintenance process

where fatigue, environmental and accidental damage play a major role there is a significant margin for SHM to interact as can be seen from the structure shown in Figure 67 under which the international aircraft maintenance steering group (MSG) works.

That SHM can become a core economic element with high asset structures can be easily shown for a structure such as an aircraft. Every operational hour lost on a commercial aircraft does generate cost of a few thousand Euros per hour each. Hence comparing this cost with the hourly rate of an inspector or technician does easily allow a number of twenty or more inspectors and technicians to work. Figures get even extreme when it comes to compare the cost of SHM equipment versus aircraft operability lost. As a conclusion: Operability of high asset value infrastructure is core.

In a larger study performed to analyse aircraft maintenance processes and to determine the potential of SHM within aircraft maintenance a major civil aircraft type flown worldwide had been considered (34). The maintenance process along a D-check, the major inspection an aircraft faces during its operational life, was selected and modelled with discrete event simulation to identify time critical structural items and estimate the potential benefit SHM could bring. Modelling, essentially involved mapping the workflow of steps needed to fully perform the interval and analysing the steps to flag time critical items. Generation of information required a large number of different types of documents to be studied. This started from Maintenance

Planning Documents (MPD) issued by the manufacturer. Since times for the different maintenance actions provided by the MPD are rather optimistic job cards had to be included which better reflect the local specifics of the maintainer and/or aircraft operator.

The maintenance process was modelled using a simulation tool named Arena (35) which is a discrete event simulation tool to model intervals. Arena has the ability to incorporate and analyse stochastic times easily. An estimate of the individual step times and a probability distribution for modelling is sufficient. The tool works on the basis of a graphical interface with processes to be constructed in a flow chart fashion. However initially it is important to plan the model before construction. Measuring the aircraft downtime is a key performance criterion in understanding where SHM could be used. The entity moving through the process would therefore be the aircraft. As the aircraft moves along the steps, the duration time would alter. Having the structure of the model such that the aircraft is the entity with maintenance actions as blocks does ensure that time critical items can be traced.

Each item in the D-Check was segregated into stages set by planners, and modelled in parallel as process blocks within a stage. The five stages in a D-Check can be summarised as:

- Stage 1: Removal
- Stage 2: Inspection
- Stage 3: Defect rectification and rebuild
- Stage 4: Paint
- Stage 5 : Final Checks

Figure 68 shows the structure of the D-check as modelled in an Arena model for greater clarity.

With the model established simulations could now be performed in accordance to the procedure generally described in Figure 69. This procedure can be split into six steps of which steps 1 to 3 have been already described for the D-check example above. For any structural item appearing on the critical path along step 3 an SHM solution has to be determined which is then fed back into the maintenance process (step 4) and its impact analysed by comparing the maintenance duration determined with the one achievable without SHM. This may be further varied in case alternative SHM technologies are available (step 6). Further SHM potentials might turn up in case the critical path along the maintenance process changes as a consequence of an SHM implementation and further components with SHM potential might turn up.

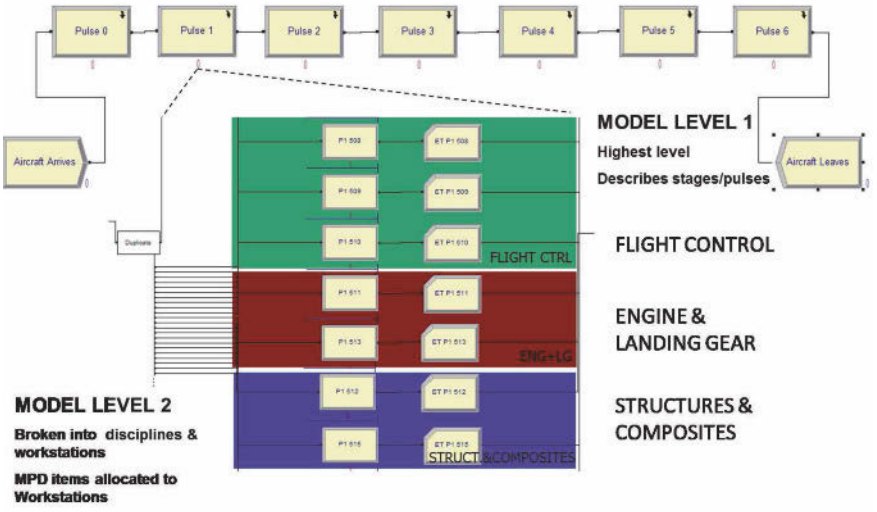

Figure 68. Structure of the D-check model. Level 1 shows the stages. A section of stage 1 has been expanded to show level 2. Here items are broken in parallel to work stations.

Maintenance work along the D-check mentioned above was organised in terms of so called process blocks. These process blocks have been the result of an optimisation of the maintenance process. Figure 70 shows the histogram for all process blocks that were considered critical. The number of hits represents the number of times a process block became critical in 100 replications, which is a result of some uncertainties specifically applied to the simulation model. The critical blocks were therefore altered due to uncertainties elicited from maintenance planners. The process blocks where SHM could be implemented are highlighted. At those process blocks there were a number of SHM solutions inapplicable (non inspections, larger visual checks) since items to be inspected required identical access. Therefore, this access would be necessary even if a SHM alternative was made available. For this reason, time savings were mainly marginal.

Figure 71 shows that the average saving between the existing process and the improved process with SHM at hot spot locations resulted in average savings of nearly 3 hours per interval. The average total saving was less than the minimum saving, as the highlighted critical process blocks were not critical 100% of the time when running the replications. Considering

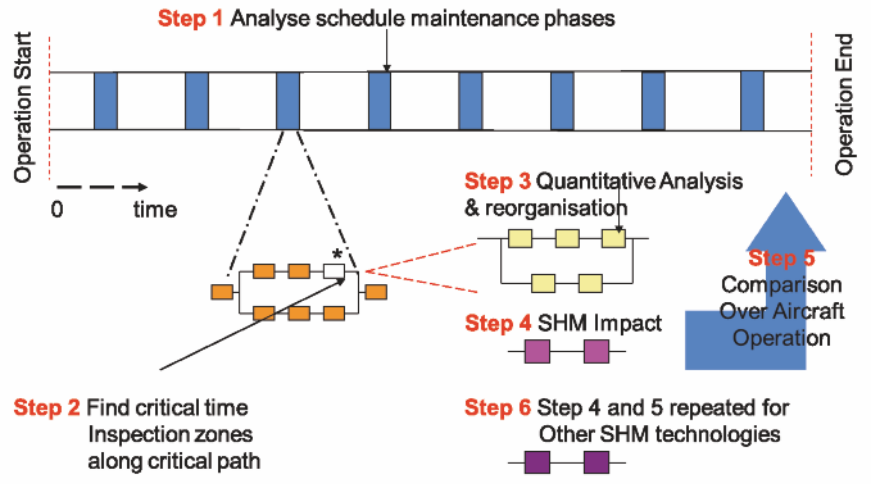

Figure 69. Procedure for analysing operational life cycle SHM potentials along the maintenance process of en engineering system

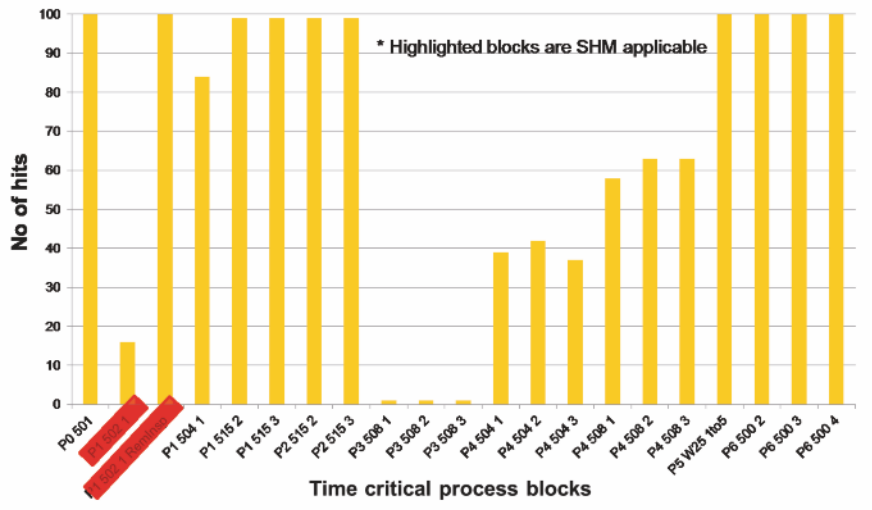

Figure 70. Number of times a process block is critical after 100 replications of D-Check simulation considering uncertainties. Highlighted blocks are where SHM is applicable

	AV. tot time hrs	Min hrs	Max hrs
Existing	413.54	371.78	460.83
SHM hot spots	410.61	367.18	451.39
SHM global	387.34	341.85	424.75
Savings	26.2	29.93	36.08

Figure 71. Comparison of the two simulation durations: one modelling the existing process and the other replicating if identified hot spot regions were eliminated.

replacement for only a handful of hot spot areas in a D-Check would yield very small savings only. The gain sought in operational capability would not even improve significantly if all structural components were equipped with SHM which is the scenario denoted as 'SHM global' in Figure 71 below. Even here the difference might not exceed 36 hrs. which is a marginal number when keeping the uncertainty and the D-check as a possibly singular event in an aircraft's life in mind. What those figures provide is the perfect match between engineering design and maintenance or in other words, aircraft structures today are designed for being well maintained. Should maintenance principles therefore change then those would most likely also have a significant implication on design. Implementing SHM into aircraft designed today or in the past is therefore most likely not to provide the expected benefits.

A major question now emerging as a consequence of the conclusion made above is now: Can SHM have a benefit for current aircraft at all? The answer to that question is 'yes' and the potentials have to be seen in something called 'drop out'. A drop-out is a damaging situation which occurs unexpectedly over an aircraft's operational life. An example is repairs, which are often not predictable and do require specific care over the aircraft's remaining life. Other drop outs are damages which occur while an aircraft is ageing and which could not be predicted before. Drop outs are most likely to define their own inspection intervals and as such those intervals are most likely not to match with the optimised maintenance plans mentioned above. Hence inspections will have to be performed with regards to those drop outs only and this may result in a fairly expensive inspection action. An example where such an SHM impact could be validated has been the gantries on the Airbus A300. Gantries as shown in Figure 72 are the major longitudinal

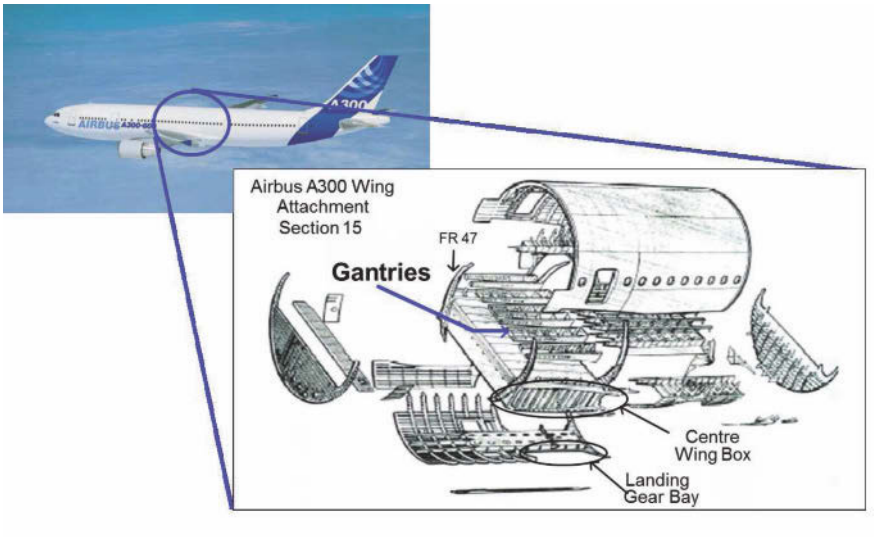

Figure 72. Drop out item gantries and its location within the aircraft

beams over the wing box of an aircraft. They are exposed to major bending loads of the aircraft fuselage as well as cabin pressure loads, which are downloaded from bolted diaphragm panels into the flanges of the gantries. The complexity of stress states in that region may result in cracks to emerge which need to be detected through inspection and be removed at intervals most likely not to be in line with the conventional maintenance process. Getting those locations inspected also requires a substantial amount of dis- and re-assembly of various components in the near-field.

In the case of gantries' inspection the process was simulated with Arena initially by varying the numbers of inspectors and workers being involved in the inspection process. Results obtained are shown in Figure 73 and it can be seen by increasing the number of workers and inspectors that the duration for inspecting the gantries will decrease, however not below a threshold value of around 120 hrs of maintenance. This result has been compared to a solution where an SHM system has been implemented around the locations prone to cracking as shown in Figure 74. This solution would only require a plug to be contacted for inspection in the aircraft's floor and would avoid any disassembly of seats, carpets, floors and possibly more. Inspection time would be reduced to 20 hours for an aircraft's remaining life cycle resulting in around 100 hours per aircraft of operability gained or

Model	Number of MRB Workers	Number of Inspectors	Total Number of Workers	Total Maintenance Time for whole life-cycle (hrs)
1	3	2	5	264.47
2	6	4	10	171.33
3	9	6	15	145.90
4	12	8	20	128.99
5	15	10	25	121.75

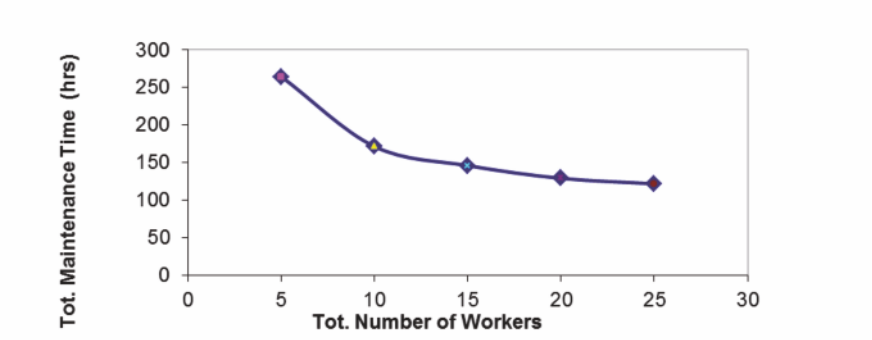

Figure 73. Total life cycle maintenance time for gantries' inspection depending on labour involved

a significant six digit Euro volume of operational cost.

SHM has its short term benefits therefore specifically in automating unscheduled inspection processes. This requires flexible solutions being application tailored. Implementing SHM at a product's life cycle onset requires the product's design principles to be modified such that an overall economic benefit can be seen. This approach is definitely only possible with products being designed from scratch but hardly from those existing today.

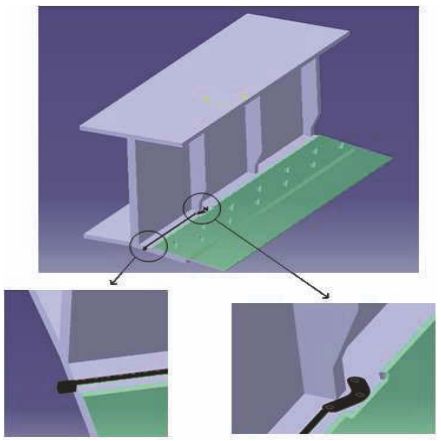

Figure 74. SHM solution considered for gantries' inspection

7 Emerging SHM Applications and Concluding Remarks

There has been a large amount of research and development done in the area of SHM. However not too much has been shown so far that has matured to a true commercial SHM product being applied. This may result from the fact that most of the areas being addressed for SHM would this be aeronautics, mechanical and/or civil engineering are disciplines being well established in engineering. Design principles would therefore have to be changed if SHM was to be implemented at the onset of a product's life cycle.

An area where design principles are much less established and where consequently technology pull plays a much bigger role is wind energy generation. Wind energy rotor blades are critical components in many regards and monitoring their loads, condition and hence damage is significant. In view of their size and limited access they are ideal for SHM applications. Along some longer standing development an SHM system is on its way to be realised (36) that is a part of a wind energy rotor blade design process and can be integrated and updated in accordance to the rotor blade's operational needs. Starting from numerical simulation locations for sensors have been determined as shown in Figure 75 below. With a hardware acoustic system which is able to work on a wireless basis acoustic signals can be generated and/or recorded which allow the relatively large allowable dam-

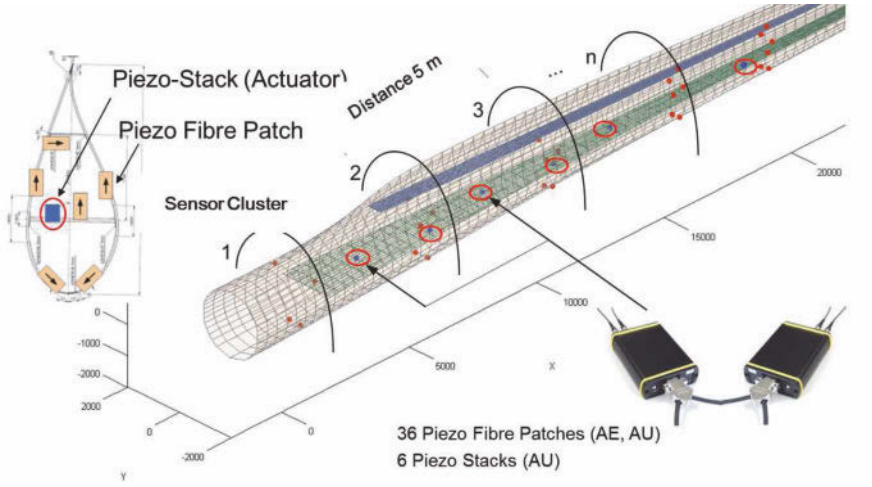

Figure 75. Numeric simulation for SHM system configuration (36)

ages to be observed in a rotor blade. Techniques considered are acoustics based including acoustic emission and acousto-ultrasonics. An additional option is provided through a fibre optic Bragg grating sensing system which allows modal shapes of the rotor blade to be monitored as an additional monitoring technique. Figure 76 shows the correlation coefficient of defined acousto-ultrasonic paths where the actual signal has been correlated with the signal from the pristine stage and a lack in correlation is considered as the damage indicator. Transducers placed in the rotor blade have also been used as sensors for acoustic emission monitoring only where damages in the rotor blade have been clearly identified as can be seen from some of the results shown in Figure 77.

Implementing SHM into wind energy systems in general is a most rewarding application for SHM technology demonstration. Components to be inspected are comparatively large and difficult to inspect. So far there are no certified inspection techniques and procedures available which give SHM a chance to become one of them. Allowable damages are relatively large when compared to aircraft and shutdown times relatively short, which is another advantage for getting SHM implemented. However there are also some challenges still to be met where lightning strikes is one of the major ones besides energy harvesting, environmental ruggedness and longevity of the SHM system which all can be nicely demonstrated on the wind energy turbine blades themselves. Challenges have also to be seen in the sensors'

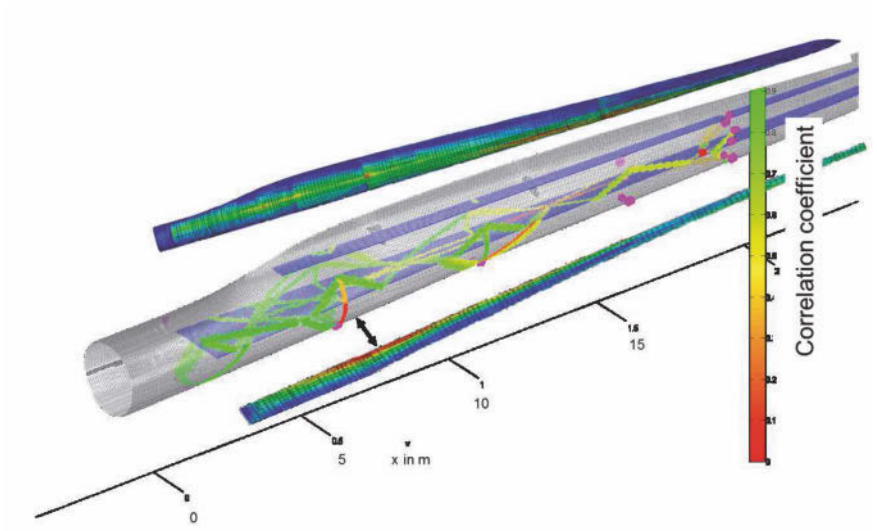

Figure 76. Acousto-ultrasonic signal correlation coefficient as a means for damage detection (36)

damage detection performance. Sensor algorithms do have to distinguish between real damage and other effects such as resulting from environmental, system failure or other external influences. SHM systems do also have to provide very high probability of damage detection capabilities which also results from an SHM system's high system integrity with basically no false positives being provided. Validation of the SHM system has also to be performed under the various environmental conditions the system has to operate in resulting in adequate SHM systems to be finally provided on the market.

Other major issues include sensor durability and a possible option for a SHM system repair. Slow or long-term damage progression resulting from corrosion, fatigue cracking, etc. has to be considered as well. A sensor/SHM system must therefore be robust to survive well beyond any of those damaging events. Repair as well as replacement of the SHM system has to be low-cost with the SHM system still being able to meet original detection requirements. SHM systems must not interfere with structural repairs or do have to be configured such that they do circumvent those or possibly even get those included.

The reasons why not too much SHM has been applied in aeronautics are

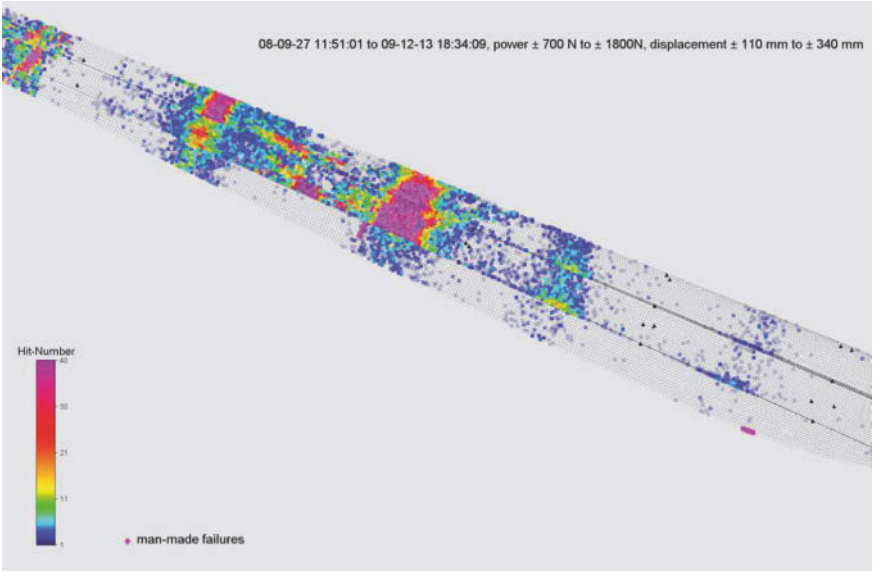

Figure 77. Localisation of acoustic emissions in wind energy rotor blade (36)

various and do include significantly the insufficient technology readiness of most of the SHM techniques proposed. Another reason is also that SHM potentials are still hardly explored and hence mainly unknown specifically from a quantitative point of view. Aircraft manufacturers mainly consider SHM within the context of new aircraft, where potentials can only be seen in very dedicated applications such as collision monitoring around cargo doors. Current and hence short term potentials are however more with ageing aircraft which is a different segment of business in which aircraft maintenance companies are more active. However those companies are reluctant to adopt SHM as a future technology since it automates current inspection processes reducing the value of maintenance business ongoing. Aircraft operators are also not aware of SHM and the SHM potentials which can only be determined once the operational conditions of their aircraft are known. However aircraft operators might be reluctant to release this information. Furthermore they are reluctant in getting more sensors on board their aircraft since they already feel sufficiently penalised with all the other sensor systems being on board ranging from avionics to wellbeing and entertainment. Airworthiness authorities could be better integrated into the SHM develop-

ment process at present although they are finally the institutions declaring an SHM system to be airworthy. Airworthiness certification may therefore become another stumbling stone along the way to get SHM into operation. Then there is the wide field of data integration. The amount of data an SHM system generates is huge and will have to be included in a data management system. In aviation data management is already a major issue within the context of avionics, flight performance and systems such as engines, landing gear, fuel and others. Data formats at any of the interfaces have already been fixed and likelihood is more than low that those will be changed or adapted with regard to SHM. Hence data generated by SHM will have to be adapted to the formats being already set in aviation so far. Finally there is too little appreciation from the 'SHM-community' with respect to activities happening in neighbouring fields. There are engine condition monitoring systems operating with success now and the same can be mentioned for the health and usage monitoring systems (HUMS) in helicopters or any type of built-in test equipment (BITE) applies in avionics.

With all this critique said there is however a variety of things that can be done straight away to get SHM realised already today. It starts with implementing loads monitoring at discrete locations and feeding the information recorded back into the fatigue life evaluation process. In a time where most of our engineering systems are designed digitally there exists a digital model that may allow for predicting damage critical locations based on the operational loads the system is going through. In a damage tolerant structure there are many components which allow for fairly large damages going far into the multi-centimetre range such as broken stringers. These damages are quite easy to detect with the SHM techniques being available provided the techniques do withstand all other environmental requirements being set. Maintenance processes can be easily simulated today which allow the potentials of SHM to be determined on a completely numerical basis before investing into SHM hardware to be realised. And last but not least one can automate the inspection process as much as possible because a human generating in nearly 100% of the cases the information 'no failure found' (NFF) gets easily bored. It would be much more beneficial having an automated inspection system filtering out most of the NFF cases and providing a residual of borderline cases which the human brain might be better challenged to tackle with since a human's capabilities in correlation are still beyond any machine as long as being challenged adequately.

Bibliography

[1] Günther G, 1993, DASA (now Cassidian) (private communication)

[2] Boller C, F-K Chang and Y Fujino (Ed.s), 2009: *Encyclopedia of Structural Health Monitoring*; 5 Volumes; John Wiley & Sons

[3] Armitag S R and D M Holford, 1998: Future Fatigue Monitoring Systems; NATO RTO AVT Proc. 7 (RTO MP-7), Paper 2

[4] Haibach E, 2006: *Betriebsfestigkeit;* Springer-Verlag, 3^{rd} Edition (in German)

[5] Matsuishi M and T Endo, 1968: Fatigue of metals subjected to varying stress – Fatigue lives under random loading; Preliminary Proc. of JSME Kyushu District Meeting, pp. 37-40 (in Japanese)

[6] Potter J M and R T Watanabe (Ed.s), 1989: *Development of Fatigue Loading Spectra,* ASTM STP 1006

[7] de Jonge J B, D Schütz, H Lowak and J Schijve, 1973: *A standardized load sequence for flight simulation tests on transport aircraft wing structures;* Nat. Aerospace Lab. (NLR) technical report TR 72018 and Fraunhofer LBF report FB-106

[8] Fischer R, M Hück, H-G Köbler and W Schütz, 1970: *Eine dem stationären Gaußprozess verwandte Beanspruchungs-Zeit-Funktion für Betriebsfestigkeitsversuche;* Fortschr.-Ber. VDI-Z Reihe 5, Nr. 30 (in German)

[9] Peterson R E, 1974: *Stress Concentration Factors,* John Wiley & Sons, New York

[10] MIL-Handbook 5J: http://femci.gsfc.nasa.gov/links.html (last visited 03/12)

[11] Palmgren A, 1924: Die Lebensdauer von Kugellagern, VDI-Z 58, pp. 339-341 (in German)

[12] Miner M A, 1945: Cumulative damage in fatigue, J. Appl. Mech., 12, pp. 159-164

[13] Schmidt H-J, B Schmidt-Brandecker and G Tober, 1999 : Design of Modern Aircraft Structure and the Role of NDI, Proc. of 7^{th} ECNDT, Vol. 4, Nr. 6 (also available on [41])

[14] Tada H, P C Paris and G R Irwin, 1973: *The stress analysis of cracks handbook*; Del Research

[15] Sih G C, 1973: *Handbook of stress intensity factors*, Lehigh University Press

[16] Rooke D P and D.J. Cartwright, 1976: *Compendium of stress intensity factors*, Her Majesty‘s Stationery Office

[17] Murakami Y, *Stress Intensity Factors Handbook*, Japan Soc. Mater. Sci., Tokyo/Japan

[18] Paris P C and F Erdogan, 1963: A critical analysis of crack propagation laws; Trans. ASME, Series D, Vo. 85, pp 528-535

[19] Forman R G, V E Kearney and R M Engle, 1967: Numerical analysis of crack propagation in cyclic-loaded structures; J. Basic Engrg., Trans. ASME, Vol. D89, pp. 459-464
[20] Grandt Jr. A F, 2004: *Fundamentals of Structural Integrity*, John Wiley & Sons
[21] Cullity B D, 1972: *Introduction to magnetic materials*, Addison Wesley, London
[22] Jiles D C, 1988: Review of magnetic methods for non-destructive evaluation, NDT International, vol. 21, 311
[23] Altpeter I, G Dobmann, M Kröning, M Rabung and S Szielasko, 2009: Micro-magnetic evaluation of micro residual stresses of the IInd and IIIrd order, NDT & E International, Vol. 42, Issue 4, pp 283-290
[24] Tiitto S, 1996: Magnetic Methods. Handbook of measurement of residual stresses; J Lu (Ed.), Soc. for Experimental Mechanics; The Fairmont Press Inc Lilburn, pp 179-223
[25] Cikalova U, B Bendjus and J Schreiber, 2009: Bewertung des Spannungszustandes und der Materialschädigung von Komponenten industrieller Anlagen, Materials Testing, Vol. 51/10, pp 678-685
[26] Altpeter I, R Becker, G Dobmann, R Kern, W Theiner, A Yashan, 2002: Robust Solutions of Inverse Problems in Eletromagnetic Non-Destructive Evaluation, Inverse Problems, **18**, pp. 1907-1921
[27] Altpeter, I, G Dobmann, K-H Katerbau, M Schick, P Binkele, P Kizler and S Schmauder, 2001: Copper Precipitates in 15 NiCuMoNb 5 (WB 36) Steel: Material Properties and Microstructure, Atomistic Simulation, and Micromagnetic NDE Techniques, Nuclear Engineering and Design 206, pp 337-350
[28] Yashan A, 2009: *Über die Wirbelstromprüfung und magnetische Streuflussprüfung mittels GMR-Sensoren*, Doctoral Thesis, Saarland University, Saarbrücken/Germany (in German)
[29] Schulze M, Heuer H, Küttner M, Meyendorf N, 2010: High-resolution eddy current sensor system for quality assessment of carbon fiber materials; Microsystem Technologies, Springer, Volume: 16 Issue: 5, pp 791-797
[30] Goldfine N, V Zilberstein, D Schlicker and D Grundy, 2009: Eddy-current in situ sensors for SHM, in [12], pp. 1051 - 1064
[31] Schütz W, 1989: *Standardized stress-time histories: An overview.* Development of Fatigue Load Spectra, ASTM STP 1006, pp. 3-16
[32] Boller C and W J Staszewski, 2003: *Aircraft Structural Health and Usage Monitoring;* in [38], pp. 29-73
[33] Boller C and M R Mofakhami, 2008: *From Structural Mechanics to Inspection Processes: Getting Structural Health Monitoring into Application for Riveted Metallic Structures*; in B Dattaguru, S Gopalakrishnan and V K Aatre(Ed.s.): IUTAM Symposium on Multi-Functional

Material Structures and Systems; IUTAM Bookseries Vol 19, Springer, pp. 175-184

[34] Kapoor H, C Braun and C Boller, 2010: Modelling and optimisation of maintenance intervals to realise Structural Health Monitoring applications on aircraft; Proc. of 5^{th} European Workshop on Structural Health Monitoring

[35] Kelton D., Sadowski P., and Sadowski A., 2002: *Simulation with Arena*, McGraw-Hill

[36] Frankenstein B, L Schubert, B Weihnacht, E Schulze, C Ebert, H Friedmann and T Granert, 2009: Development of condition monitoring systems for rotor blades of windmills; Prof. of 7^{th} Internat. Workshop on SHM, DESTech Publ., pp. 1595-1602

Further Reading:

[37] Niu M C Y, 2002: Airframe Structural Design, Hong Kong Conmilit Press Ltd., 2nd Edition

[38] Staszewski W J, C Boller and G R Tomlinson, 2003: Health Monitoring of Aerospace Structures; J. Wiley & Sons

[39] Broek D, 1989: The Practical Use of Fracture Mechanics; Kluwer Academic Publ., Dordrecht, Netherlands

[40] Dowling N, 1998: Mechanical Behaviour of Materials, Prentice Hall

[41] Non-destructive testing: http://www.ndt-ed.org/index_flash.htm or http://www.ndt.net (last visited 03/12)

[42] Bray D and R K Stanley, 1989: Nondestructive Evaluation; McGraw Hill

[43] Aircraft accidental reports: http://www.ntsb.gov (last visited 03/12)

[44] Crack propagation software AFGROW http://www.afgrow.net (last visited 03/12)

[45] The Damage Tolerance Design Handbook http://www.afgrow.net/applications/DTDHandbook/pdfs.aspx (last visited 03/12)

[46] Balageas D, C-P Fritzen and A Güemes, 2006: *Structural Health Monitoring*, ISTE Ltd.